◆ Human Brain Mapping 33:2005–2034 (2012) ◆

Probabilistic Tractography Recovers a Rostrocaudal Trajectory of Connectivity Variability in the Human Insular Cortex

Leonardo Cerliani,[1,2,3]* Rajat M. Thomas,[4] Saad Jbabdi,[5] Jeroen C.W. Siero,[1,2,6] Luca Nanetti,[1,2] Alessandro Crippa,[1,2,7] Valeria Gazzola,[1,2,3] Helen D'Arceuil,[8] and Christian Keysers[1,2,3]

[1]*BCN NeuroImaging Center, University of Groningen, A. Deusinglaan, 2-9713AW Groningen, The Netherlands*
[2]*Department of Neuroscience, University Medical Center Groningen, A. Deusinglaan, 2-9713AW Groningen, The Netherlands*
[3]*Social Brain Laboratory, Netherlands Institute for Neuroscience, Royal Netherlands Academy of Arts and Sciences, Amsterdam, The Netherlands*
[4]*Kapteyn Astronomical Institute, Faculty of Mathematics and Natural Sciences, University of Groningen, 9700AV Groningen, The Netherlands*
[5]*Oxford Centre for Functional Magnetic Resonance Imaging of the Brain (FMRIB), Department of Clinical Neurology, University of Oxford, United Kingdom*
[6]*Department of Radiology, University Medical Center Utrecht, Utrecht, The Netherlands*
[7]*Scientific Visualization and Computer Graphics Group, Institute for Mathematics and Computing Science, University of Groningen, PO Box 800, 9700AV Groningen, The Netherlands*
[8]*Department of Radiology, Athinoula A. Martinos Center for Biomedical Imaging, Massachusetts General Hospital, Harvard Medical School, Charlestown, MA 02129*

Abstract: The insular cortex of macaques has a wide spectrum of anatomical connections whose distribution is related to its heterogeneous cytoarchitecture. Although there is evidence of a similar cytoarchitectural arrangement in humans, the anatomical connectivity of the insula in the human brain has not yet been investigated in vivo. In the present work, we used in vivo probabilistic white-matter tractography and Laplacian eigenmaps (LE) to study the variation of connectivity patterns across insular territories in humans. In each subject and hemisphere, we recovered a rostrocaudal trajectory of connectivity variation ranging from the anterior dorsal and ventral insula to the dorsal caudal part of the long insular gyri. LE suggested that regional transitions among tractography patterns in the insula occur more gradually than in other brain regions. In particular, the change in tractography patterns was more gradual in the insula than in the medial premotor region, where a sharp transition between

Additional supporting information may be found in the online version of this article.

Saad Jbabdi and Jeroen C.W. Siero contributed equally to this work.

Contract grant sponsor: Nederlandse Organisatie voor Wetenschappelijk Onderzoek (NWO) Cognitive Pilot Project; Contract grant number: 051.07.003; Contract grant sponsor: NWO VIDI; Contract grant number: 452-04-305; Contract grant sponsor: NWO MaGW; Contract grant number: 400-08-089; Contract grant sponsor: Marie Curie Excellence Grant; Contract grant number: MEXT-CT-2005-023253.

*Correspondence to: Leonardo Cerliani, Department of Neuroscience, BCN NeuroImaging Center, University Medical Center Groningen, Antonius Deusinglaan, 2-9713AW Groningen, The Netherlands. E-mail: leonardo.cerliani@gmail.com

Received for publication 28 July 2010; Revised 28 March 2011; Accepted 4 April 2011

DOI: 10.1002/hbm.21338

Published online 14 July 2011 in Wiley Online Library (wileyonlinelibrary.com).

different tractography patterns was found. The recovered trajectory of connectivity variation in the insula suggests a relation between connectivity and cytoarchitecture in humans resembling that previously found in macaques: tractography seeds from the anterior insula were mainly found in limbic and paralimbic regions and in anterior parts of the inferior frontal gyrus, while seeds from caudal insular territories mostly reached parietal and posterior temporal cortices. Regions in the putative dysgranular insula displayed more heterogeneous connectivity patterns, with regional differences related to the proximity with either putative granular or agranular regions. *Hum Brain Mapp 33:2005–2034, 2012*.

Key words: DTI; insula; laplacian eigenmaps; diffusion-weighted imaging; connectivity-based parcellation

INTRODUCTION

Two major features characterize the anatomical organization of the insular cortex: the wide spectrum of its anatomical connections and its heterogeneous cytoarchitecture [Mesulam and Mufson, 1985]. In macaques, the insula projects to primary and secondary sensory cortices [Friedman et al., 1986; Mesulam and Mufson, 1982b; Mufson and Mesulam, 1982], to premotor regions [Luppino et al., 1993; Matelli et al., 1986], to the posterior parietal lobule [Andersen et al., 1990; Cavada and Goldman-Rakic, 1989; Rozzi et al., 2006] as well as to higher-order association areas in the prefrontal lobe [Petrides and Pandya, 1999]. The insula, especially its anterior portion, also has extensive connections with the amygdaloid complex [Amaral and Price, 1984; Mufson et al., 1981; Stefanacci and Amaral, 2002] as well as with other limbic and paralimbic regions in the frontal and temporal lobes [Cavada et al., 2000; Kondo et al., 2005; Mesulam and Mufson, 1985; Moran et al., 1987]. Insular projections were found to both limbic and motor compartments of the striatum [Chikama et al., 1997; Fudge et al., 2005] to autonomic nuclei in the brainstem and several thalamic nuclei (see Augustine [1985, 1996] and Mesulam and Mufson [1985] for extensive reviews).

The distribution of the insular cytoarchitectonics is organized radially around the limen insulae [Mesulam and Mufson, 1982a; Nieuwenhuys et al., 2008]: the anterior ventral part of the insula, coextensive with the piriform cortex and the claustrum, has an agranular structure, while the posterior dorsal part has an isocortical homotypical structure. The transitional dysgranular cortex in the anterior–dorsal, middle, and posterior–ventral insular territories shows a continuous pattern of progressive lamination with an incipient presence of granule cells in layers II and IV in the anteroventral–posterodorsal direction [Carmichael et al., 1994; Mesulam and Mufson, 1982a]. A similar architectural organization was also found in the human insula [Bonthius et al., 2005; Mesulam and Mufson, 1982a; Rose, 1928; Shaw et al., 2008; Zilles, 2004] including recent observer-independent probabilistic cytoarchitectonic maps of the posterior insula [Kurth et al., 2010a].

In macaques' insula, the wide spectrum of anatomical connections and the heterogeneous cytoarchitecture are related in at least two ways. First, agranular and granular regions of the insula establish preferential, though not exclusive, connections with cortical regions featuring the same architecture, while the dysgranular territory projects to regions that range from allocortex to granular isocortex. Second, the proximity of different territories in the insula dysgranular (Id) with either insula agranular (Ia), or insula granular (Ig) is reflected in their connectivity pattern, in such a way that the anterior dysgranular sector has a connectivity pattern that bears greater resemblance to that of Ia, while the connections of the posterior dysgranular insula are more similar to that of Ig [Mesulam and Mufson, 1982b, 1985].

Although these studies provided an extensive knowledge of the anatomical connections of the macaque insula, very little is known about the anatomical connectivity of the human insula. In this work, we used in vivo probabilistic tractography [Behrens et al., 2003, 2007] on diffusion-weighted (DW) magnetic resonance images to investigate the connectivity distribution of the insular cortex, where we define "connectivity distribution" as the output of probabilistic fibre tracking (see Methods, section Probabilistic Tractography for further details). Our aims were to analyze the trajectory of connectivity variation across different insular territories, to compare the results with the knowledge derived from tracer-injection studies in macaques and to evaluate whether the results would suggest a relationship between cytoarchitecture and connectivity in humans resembling that found in macaques.

Previous studies have used in vivo probabilistic tractography to successfully recover boundaries between subregions featuring sharply different connectivity patterns in the inferior frontal gyrus [IFG; Anwander et al., 2007; Klein et al., 2007], in the lateral premotor cortex [Tomassini et al., 2007], in the cingulate cortex [Beckmann et al., 2009], and between supplementary and presupplementary motor area (SMA and preSMA, respectively) in the medial premotor cortex [mPMC; Johansen-Berg et al., 2004]. In all these cases, spectral reordering or hard clustering algorithms were used, because a clear-cut subdivision was expected between subregions with different connectivity [Behrens and Johansen-Berg, 2005]. However, in the case of the insula, a general consensus about the sharpness of

the borders between subregions featuring different connectivity and cytoarchitecture is still lacking. Brodmann [1909] reported two to four main cytoarchitectural subdivisions, stressing in several occasions the fact that "there are great difficulties in dividing [the insula] into individual fields" [Brodmann, 1909: 122]. Other maps of the human insula produced in the first half of the 20th century by von Economo [1927], Rose [1928], and Brockhaus [1940] reported the presence of an anterior agranular and a posterior dysgranular sector as well as of a transitional dysgranular sector whose location and boundaries vary considerably among different maps. More recent investigations in macaques explicitly reported a gradual transition across different cytoarchitectonic fields [Friedman et al., 1986; Jones and Burton, 1976; Mesulam and Mufson, 1982a, 1985] also reflected in a gradual differentiation of the intracortical myelin [Friedman et al., 1986; Mesulam and Mufson, 1982a] and associated with a gradual transition of connectivity [Chikama et al., 1997; Mesulam and Mufson, 1982b, 1985]. On the other hand, a recent observer-independent study on 10 postmortem human brains clearly identified boundaries between different cortical types in the insular region caudal to the central insular sulcus [Kurth et al., 2010a]. Finally, at least two studies also reported a similar topographical arrangement of different cytoarchitectonic fields in humans and macaques [Bonthius et al., 2005; Mesulam and Mufson, 1982a].

Given the available anatomical evidence, applying a hard-clustering technique in the insula would be undesirable, as it would, by definition, split the insula in discrete clusters without first assessing whether the data indeed suggest the presence of homogeneous clusters separated by sudden changes of connectivity. In a previous study [Nanetti et al., 2009], we showed that repeated applications of *k*-means clustering reveal that the location of this border is unstable and that a large zone in the middle insula cannot be reliably classified using *k*-means. Therefore, we resort here to the use of a nonlinear dimensionality reduction technique, Laplacian eigenmaps (LE) [Belkin and Niyogi, 2002], to represent insular voxels as points on a plane, in such a way that the distance between each pair of voxels would quantify the similarity of their respective connectivity maps. This technique is similar to the spectral reordering algorithm previously used in other connectivity-based parcellation studies [Johansen-Berg et al., 2004, 2008; Klein et al., 2007], but it also takes advantage of the information about the nearest neighbors of each connectivity feature vector. Considering the spatial arrangement of the seed voxels according to the LE of their tractography feature vectors allowed us to investigate whether connectivity varies gradually across the insula or whether it is characterized by the presence of sharply delimited clusters.

LE of the insular connectivity maps reveals a main trajectory of connectivity variation along the rostrocaudal anatomical axis, spanning from the most anterior insula, encompassing the anterior short gyrus as well as the ventral anterior insula around the limen, to the dorsal and posterior part of the long gyri. The distribution of the brain regions reached by fiber tracking seeded in different insular territories is mostly in agreement with tracer-injection studies in macaques and suggests a relationship with the cytoarchitecture. Finally, LE reveals significant differences in the structure of connection variability when comparing insula and mPMC: sharp changes in connectivity were detected in the mPMC, while in the case of the insula, the connectivity variability was organized in a more continuous manner along the identified rostrocaudal axis.

MATERIALS AND METHODS

Ten healthy adult males (median age, 35; range, 27–50) took part in the experiment. Limb dominance was assessed with a dutch translation of the Edinburgh Handedness Inventory [Oldfield, 1971]. All participants were right-handed (all scores above 60/100).

The participants gave informed written consent in accordance with the Declaration of Helsinki and with the study protocol, which was approved by the Medical Ethical Commission (METc) of the University Medical Center Groningen (NL).

Image Acquisition and Preprocessing

DW data were acquired using a single-shot pulsed gradient spin echo EPI sequence (TR = 7,500 ms, TE = 67 ms, and SENSE factor = 2) on a 3-T MR scanner (Intera, Philips Medical Systems, Best, the Netherlands) equipped with an eight-channel head coil. For each subject, 15 DW images were collected using the "medium" gradient scheme provided by the manufacturer, with a maximum gradient strength of 22 mT m^{-1} and a *b*-value of 1,000 s mm^{-2}. In addition, one non-DW volume ($b = 0$ s mm^{-2}, referred in the following as a *b*0 image) was acquired. Each volume consisted of 76 transverse slices, acquired with a 96 × 96 matrix (FOV = 224 × 224 mm, voxel size = 2.3 × 2.3 mm, slice thickness 2 mm, no gap; reconstructed matrix 128 × 128 leading to a final resolution of 1.75 × 1.75 × 2 mm^3; NEX = 2). The total acquisition time for this sequence was 4 min and 14 s. In addition, one high-resolution (1 mm isotropic) 3D anatomical scan (T1W, TFE CLEAR, TR = 7,600 ms, TE = 3.6 s, and flip angle = 8°) was acquired.

All the preprocessing stages were performed by means of the software provided with FSL 4.1.1 [Smith et al., 2004; Woolrich et al., 2009] (available at www.fmrib.ox.ac.uk/fsl). Preprocessing of DW images involved realigning all the DW volumes to the *b*0 to correct for movements and for eddy currents. Subsequently, the skull was automatically removed from both the *b*0 and the anatomical scan using Brain Extraction Tool [Smith, 2002], and the *b*0 was registered to the anatomical scan [affine registration, 7

degrees of freedom (DOF)] and to the MNI template (affine registration, 12 DOF, target voxel resolution: 2 × 2 × 2 mm) by means of FLIRT [Jenkinson et al., 2002].

Definition of the Insular Region of Interest

The insular cortex was drawn on the anatomical image realigned to the *b*0 and taken into the corresponding resolution, using the inverse of the previously calculated matrix to register the *b*0 to the T1-weighted image. The location of the drawn ROIs was later inspected by overlaying them onto the *b*0 image. A study from Naidich [Naidich et al., 2004] showed the reliability of MR images to identify anatomical landmarks for the insular region. We rely on the landmarks described in that work to draw our ROI, using the terminology mediated by Türe et al. [1999] (see Fig. 1).

The anterior limit of the insula was identified in the anterior periinsular sulcus, at the level of the junction between the internal and external capsule, extending ventrally until the subapical insular pole. The posterior limit was the most dorsocaudal extent of the anterior long gyrus of the insula. The superior periinsular sulcus was defined the dorsal boundary of the ROI. Ventrally and caudally, the inferior periinsular sulcus (IPS) was drawn in posterior-to-anterior direction, as far as the junction with the temporal operculum (at the level of the limen insulae). No anatomical landmark can be used to delimit the insular cortex from the adjacent posterior orbitofrontal cortex [OFC; Heimer and Van Hoesen, 2006; Mesulam and Mufson, 1982a, 1985]; therefore rostral to the limen insulae, we chose the ideal plane connecting the insular pole with the most rostral location where the junction with the the temporal operculum could be identified in order to draw the anterior–ventral boundary. Laterally, the insula was delimited by the CSF, while medially we chose those voxels at the interface with the underlying white matter as a boundary of the seed region. Given the limits imposed by the voxel resolution as well as by the morphology of the ventral insular cortex with respect to the claustrum, it is possible that some voxels in the ventral insular ROI may include some part of the claustrum (see Discussion: A Comment on the Claustrum).

Probabilistic Tractography

Probabilistic fiber tracking was performed with the FMRIB's diffusion toolbox [Behrens et al., 2003] from each insular voxel to the ipsilateral hemisphere using a model that accounts for the presence of either one or two fibers in each voxel [Behrens et al., 2007]: at each step, during the fiber-tracking process, a fiber orientation was chosen from each of the estimated fiber populations supported by the data, and the pathway was tracked along the fiber orientation closest to the one chosen in the previous tracking step; pathways looping back on

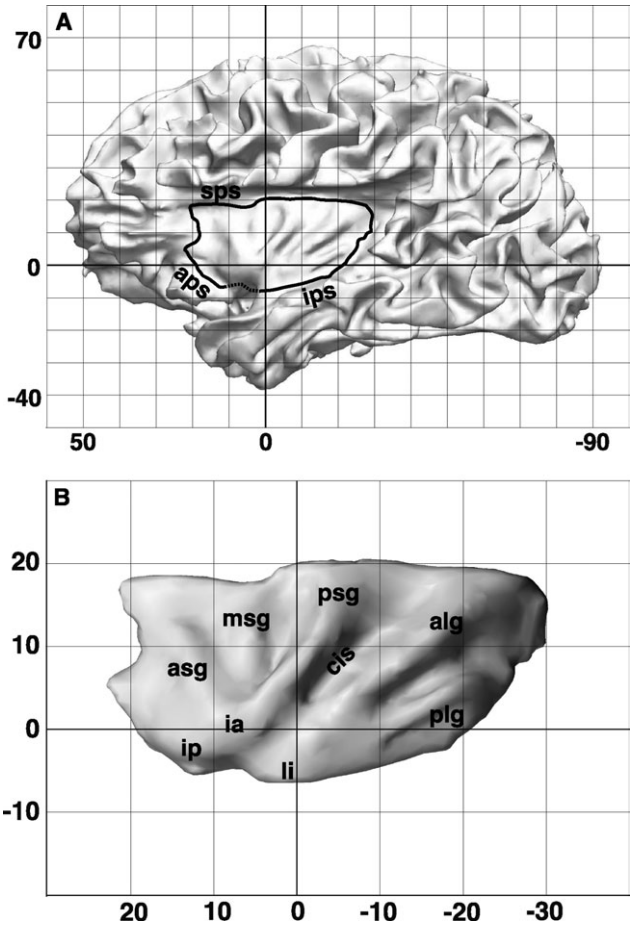

Figure 1.

Definition of the insula ROI. **A**: Surface rendering of the left brain in one subject at approximately mid-way through the cortical gray matter (cortical layer 4) [Van Essen, 2005]. The coordinates (0,0) indicate the *Y* and *Z* location of the anterior commissure (AC). Large parts of the frontal, parietal, and temporal opercula were removed to show the location of the insula and the landmarks chosen to draw the ROI: anterior periinsular sulcus (aps), superior periinsular sulcus (sps), and inferior periinsular sulcus (ips). The dotted line connecting the limen insulae (li) with the insular pole (ip) represents the ideal boundary between the anterior ventral insula and the posterior orbitofrontal cortex. A detailed description of the drawing of the insula ROI in the subjects' volumes is provided in the main text. B: Surface rendering of the insular cortex in the same subject. This subject was chosen to show the morphology of the insula, because it presents the most common configuration of the short and long gyri according to the dissection studies conducted by Türe [1999]. Abbreviations: alg, anterior long gyrus; aps, anterior periinsular sulcus; asg, anterior short gyrus; cis, central insular sulcus; ia, insular apex; ip, insular pole; ips, inferior periinsular sulcus; li, limen insulae; msg, middle short gyrus; plg, posterior long gyrus; psg, posterior short gyrus; sps, superior periinsular sulcus.

themselves were terminated. Five thousand samples were drawn from the connectivity distribution of each seed voxel, yielding a connectivity map recording the location of the target voxels reached by probabilistic tractography as well as the number of samples crossing each target voxel. These values were further multiplied by the mean length of the pathways connecting each seed with each target voxel [Beckmann et al., 2009; Eickhoff et al., 2010; Tomassini et al., 2007] to ensure that the results of tractography, and the following calculation of similarity between connectivity maps, were not biased toward nearby connections due to the mere anatomical proximity.

It is important to specify how we will frame the results of probabilistic tractography in the context of studying the anatomical connectivity of the insular cortex. In the following, we will refer to the results of probabilistic tractography as "connectivity maps" and to the samples sent from a seed voxel to a target voxel as "projections." The proper use of these terms belongs to the realm of animal studies, in which tracers can be injected in specific brain regions to label axonal pathways, distinguish afferents and efferents, and stain single neural termination. In MR tractography, is it not possible to achieve this level of resolution; we can only infer the location and shape of entire white-matter bundles from the effect of the displacement of water molecules on the MR signal at the voxel level, estimate the uncertainty associated with this signal, and finally calculate a distribution of possible directions to follow during tractography. Therefore, when discussing the results of probabilistic tractography of the insula, we will use the term "projections" to refer to those voxels in the brain where samples were recorded after performing probabilistic tractography from a given seed voxel or seed region, the location of these samples in the brain being represented by a "connectivity map." In doing so, we comply with previous connectivity-based parcellation studies [Behrens et al., 2003; Croxson et al., 2005; Rushworth et al., 2006; Tomassini et al., 2007] in which terms such as "connectivity" and "projections" were used to describe the results of probabilistic tractography after strict definitions of the terminology.

LE of the Insula

Because we aimed at analyzing the structure of the connectivity variability across insular seed voxels, we first needed a quantitative description of the similarity between the connectivity map of each and every other seed voxel. The similarity between the connectivity maps of two seed voxels was quantified in terms of the location of the target voxels in the brain reached during probabilistic tractography as well as by the number of samples reaching each target voxel. This part of the procedure has been detailed in previous works [Anwander et al., 2007; Beckmann et al., 2009; Johansen-Berg et al., 2004; Klein et al., 2007; Tomassini et al., 2007]. In brief, for every subject and every hemisphere, the connectivity map of each seed voxel was reshaped in a vector of length equal to the number of voxels in the ipsilateral hemisphere. After reducing the dynamic range of the values by logarithmic transformation [Anwander et al., 2007], the similarity between each two (vectorized) connectivity maps, calculated using the Pearson correlation coefficient, was stored in a square matrix A of dimensions $n \times n$, where n is the number of seed voxels in the insula of each subject. Each row (or column) of the matrix is therefore a feature vector for one seed voxel, representing the similarity between that voxel's connectivity map and the connectivity map of every other seed voxel (Fig. 2, left).

The final aim in building this matrix is to group together seed voxels with similar connectivity maps. However, two connectivity maps can be highly correlated because of the connections between their respective seed voxel, instead of the connections with brain regions outside the seed mask, which are the most interesting for connectivity-based parcellation studies. To correct for this bias, we added to the matrix A an euclidean distance matrix of the anatomical distance across the seed voxels (scaled in the range 0..1 on a single subject basis). In this way, the similarity between two connection probability maps is reduced as a function of their anatomical proximity. The resulting matrix of the feature vectors was then fed into the algorithm of the LE [Belkin and Niyogi, 2002] to analyze the trajectory of connection variability across insular territories.

LE [Belkin and Niyogi, 2002] was used to recover, if present, a structure of connectivity variability across all seed voxels' connectivity maps. A technical exposition of the implementation of LE for probabilistic tractography data is provided in the Supporting Information. In brief, the algorithm uses the information about each feature vector's nearest neighbours—that is, those vectors with the smallest euclidean distance to a given vector—to map the feature vectors, which are originally points in R^n (a space in n dimensions) as points in R^2 (a plane), so that the proximity in R^2 reflects the proximity in R^n. A graph was calculated from the matrix A, connecting each two feature vectors whose Eluclidean distance was less or equal than the distance required for the graph to be connected. The Laplacian matrix of this graph was computed, and the eigenvectors associated with the first two smallest nonzero eigenvalues of the Laplacian matrix (first and second component in Fig. 2, middle) were used to map the connectivity feature vectors of each seed voxel as points on a plane. If the connectivity across insular regions varies in a continuous manner between two extremes with highly different connectivity patterns, we expected the algorithm to arrange the seeds along a line. On the other hand, if the insula features subregions with sharply different connectivity among each other, we expected the algorithm to detect large interruptions on the line or segregated clouds of points.

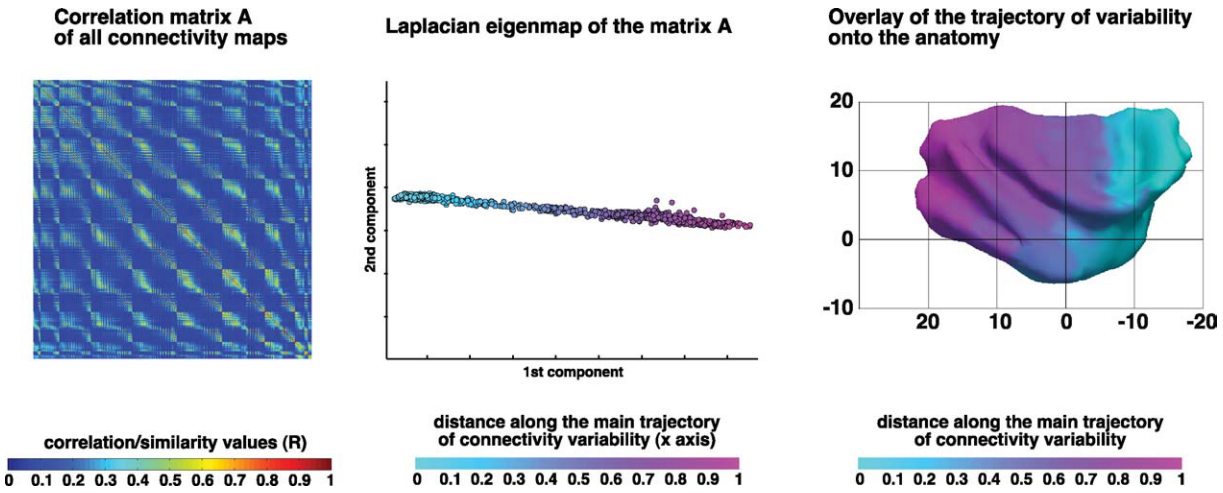

Figure 2.

Computation of the Laplacian eigenmap of the insular connectivity feature vectors in a single subject. Left column: Similarity matrix A, containing the correlation values between each and every other seed voxel's connectivity maps calculated by probabilistic tractography. Colors indicate the value of the Pearson correlation coefficient *R*. Middle column: The matrix A was fed into the algorithm of the Laplacian eigenmaps (see details in the main text and in the Supporting Information) in order to assess the presence of a structure of connectivity variability across all seeds. The algorithm maps the feature vectors, which are originally points in R^n (a space in *n* dimensions) as points in R^2 (a plane), so that the proximity in R^2 reflects the proximity in R^n. The recovered one-dimensional structure suggests to the presence of a variation between two extremes with very different connectivity, while the absence of large discontinuities (further quantified in the comparison with the medial premotor region—See Methods and Results sections: gradual versus clustered trajectory of connectivity variability, and Fig. 5) suggests that the variation of the connectivity patterns across insular voxels was gradual rather than organized in clusters with sharply different connectivity patterns. The distance from the minimum value on the *x* axis was calculated for each voxel, normalized in the range 0..1 and mapped on the anatomical surface of each subject's insula (Right column). Note that the distances in the Laplacian eigenmap only reflect distances across feature vectors (and ultimately across the connectivity patterns of each seed voxel), while they do not reflect per se distances in millimeters in the anatomy: the topographical organization of values assigned to the seed voxels emerges only when those distances are mapped onto the anatomy. For the purposes of visualization, Caret (http://www.nitrc.org/projects/caret/) was used to segment gray and white matter and produce fiducial surface representation [Van Essen, 2005] of the insula at approximately mid-way through the cortical gray matter (cortical layer 4) [Van Essen et al., 2001]. The coordinates (0,0) indicate the *Y* and *Z* location of the anterior commissure. [Color figure can be viewed in the online issue, which is available at wileyonlinelibrary.com.]

To clarify the subsequent steps of the analysis, we need to anticipate that in all subjects, the mapping produced by LE revealed the presence of a one-dimensional structure, suggesting a trajectory of connection variability between two extremes with very different connectivity feature vectors. Importantly, higher-dimensional LE produced using three and four components did not alter the topology of the structure. The distance of each point on the line from one extreme was therefore calculated and overlaid on the anatomy of each subject (Fig. 2, right) to evaluate the topographic distribution of the recovered trajectory of connection variability. For visualization purposes, these maps were then transformed in the space of the standard MNI template (affine transformation, 12DOF, and nearest neighbour interpolation), and the median value for each insular voxel belonging to at least five subjects (half of the participants) was calculated in order to produce a map of the average trajectory of connectivity variability in the insula across subjects. By considering only the voxels in MNI space that belonged to at least five subjects, we achieved the best approximation to the location and boundary of the insula as they appear in the ICBM152 brain template (http://www.loni.ucla.edu/ICBM/). To evaluate the topographic distribution of insular connectivity in relation to the results of LE, we considered all the target voxels where 50 or more tractography samples (calculated on the connectivity maps of each seed voxel for each subject separately) had been recorded in at least half of the participants. A surface map was then computed, color-matching each region of the cortical surface to the insular territory from which the largest amount of samples, averaged over all the subjects, was recorded during tractography. To do

so, the connectivity maps of each subject were grouped in 100 bins of equal size, according to the trajectory of connection variability found by LE on a single subject basis.

Gradual Versus Clustered Trajectory of Connectivity Variability

Tracer injection studies in macaques suggest that the insula features a gradual transition of anatomical connectivity patterns [Chikama et al., 1997; Mesulam and Mufson, 1982b], spanning the rostrocaudal anatomical axis. When considering the results of probabilistic tractography, LE can provide indications about the relative smoothness of the transition among different tractography patterns in the insula: for a given seed region, if the transition among tractography patterns is relatively smooth, the markers in the low-dimensional representation (plane) identifying different seed voxels (Fig. 2, middle) would lie on a continuous line with relatively small spatial discontinuities; on the other hand, if the examined region of interest is composed of different sharply segregated clusters, the structure of connectivity variability would display large spatial gaps among clusters. To assess which of these two configuration would better characterize the tractography results in the insula, we compared the LE of the insula with those of the mPMC, a region where both animal studies (see Luppino et al. [1993] and Picard and Strick [1996] for a review) and in vivo connectivity-based parcellation studies in humans [Anwander et al., 2007; Johansen-Berg et al., 2004; Kim et al., 2010] evidenced the presence of sharp changes across connectivity patterns. We hypothesized that LE of the mPMC would have displayed large gaps on the trajectory of connectivity variability in correspondence to the boundaries between clusters, and these gaps would have been quantitatively larger than those present in the LE of the insula.

We calculated LE of the connectivity feature vectors for the mPMC region defined in the same way as in previous connectivity-based parcellation studies [Anwander et al., 2007; Johansen-Berg et al., 2004]: one single slice on the parasagittal plane at $X(\mathrm{MNI}) = -2$, extending from $Y(\mathrm{MNI}) = -22$ to $Y(\mathrm{MNI}) = 30$ on the rostrocaudal axis and from above the cingulate sulcus to the dorsal crest of the medial wall of the hemisphere on the dorsoventral axis. The analysis was also repeated for the right hemisphere at $X(\mathrm{MNI}) = 2$. To compare the trajectories of connection variability of insula and mPMC, we calculated the distance of each point in the LE from one extreme, and after smoothing the values with a moving average (window = five points), we calculated the size of the gaps as the distance between the nth point and the $(n-1)$th point along the trajectory of connection variability. To account for the different dimensions of the insula and mPMC, the gap values for the SMA region were divided by the ratio between the size of the insula and the size of the SMA/preSMA ROI within each subject. The maximum gap was calculated as the median of the highest (1%) gap sizes: this value should inform about the presence of transitions between clusters and was therefore expected to be higher for the mPMC. This hypothesis was tested separately in each hemisphere with the Wilcoxon signed rank test.

Topographic Distribution of Insular Connection Probabilities in Relation to the Cytoarchitecture

In macaques, a strong relationship has been found between the cytoarchitecture of different insular regions and the cytoarchitecture of the regions in the brain to which they are connected [Mesulam and Mufson, 1982b, 1985; Mufson and Mesulam, 1982]. Using current neuroimaging techniques, it is still difficult to obtain a detailed in vivo quantification of the cytoarchitecture of different cortical regions (but see Eickhoff et al. [2005a,b], Fatterpekar et al. [2002], Geyer et al. [2011]). On the other side, macroanatomical landmarks do not always match with cytoarchitectonic borders [Amunts et al., 1999, 2004, 2005; Caspers et al., 2006; Geyer et al., 1999, 2000, 2004; Grefkes et al., 2001; Scheperjans et al., 2008]. The standardized probabilistic cytoarchitectonic maps available in the SPM Anatomy Toolbox [Eickhoff et al., 2005b] currently provide the best available estimation of the cytoarchitectonic distribution of several cortical regions across subjects. Among the currently mapped regions, some are particularly relevant to the study of insular connectivity, because the topographical distribution of their projections in the insula is known from animal studies, and because they span a wide spectrum of cortical types. We used the maps from the cytoarchitectonic atlas of Juelich [Eickhoff et al., 2005b] to compare the results of probabilistic tractography in the human insula with the knowledge about insular connectivity derived from tracer injection studies in macaques and to assess the relationships between the trajectory of connectivity variability recovered in the insula with probabilistic tractography, and the trajectory of cytoarchitectural variability known from animal studies.

We chose as targets the maximum probability maps (MPM, [Eickhoff et al., 2005a,b] of the probabilistic cytoarchitectonic maps for BA6 [Geyer, 2004], SI (Area 1, 2, 3a, 3b) [Geyer et al., 2000; Grefkes et al., 2001], BA44 and BA45 [Amunts et al., 1999], inferior parietal lobule (IPL: PF, PFm, PFcm, PFt, PGp, Pfop, and PGa; [Caspers et al., 2006]), superior parietal lobule (SPL: 5M, 5Ci, 5L, 7M, 7PC, 7A, and 7P; [Scheperjans et al., 2008]), and a volume, hereafter referred to as Limbic ROI comprising hippocampus (CA, FD, HATA, and SUB), amygdala (CM, SF, and LB), and enthorinal cortex (EC) [Amunts et al., 2005]. The MPM of these regions was transformed in the single-subject DW space using the inverse of the previously calculated transformation matrix taking the single-subject $b0$

image in the MNI space (affine transformation, 12DOF, and nearest neighbour interpolation), and the connection probability of each seed voxel to each target region was calculated as the proportion of the samples from the connectivity distribution of that seed, which was sent to all targets. For each target region, voxels in the insula with a connection probability lower than 0.05 were excluded from further analyses. For the purposes of visualization and qualitative estimation, the resulting seven connection probability maps for each subject were transformed into the standard MNI space (affine transformation, 12DOF, and trilinear interpolation), and the average (median) connection probability maps across subjects were calculated in all insular voxels belonging to at least half of the participants (five subjects—for the reasons previously detailed in Methods section: LE of the insula).

To investigate potential asymmetries in insular connections between right and left hemisphere, we considered separately the amount of samples sent from the insular cortex to each target, and the extent of insular cortex found to be connected to each target region. For each subject, voxels sending less than 50 samples to each target were discarded to remove potential biases of the results due to seed voxels with a low probability to be connected to the target. Differences between hemispheres in the average number of samples and in the extent of the connected insular region to each target were computed by means of paired t tests and corrected for multiple comparison with a false discovery rate of 0.05. To investigate the spatial variability of insular connections across subjects and between hemispheres, we computed maps showing for each insular voxel the number of subjects who displayed an above-threshold number of tractography samples to each of the examined targets and plotted the associated centers of gravity (COG). For each target, we also used Levene and Brown–Forsythe tests to compare the variability in the distance of every subject's COG from the mean COG between the two hemispheres.

RESULTS

LE of the Insular Cortex

In each subject and hemisphere, Laplacian eigenmaps (LE) identified a topographically organized trajectory of connectivity along the rostrocaudal axis. One extreme of this trajectory was located in the anterior insula, in a territory including the ventral anterior insula around the limen as well as the anterior short gyrus; the other extreme was located in the dorsal and caudal extent of the long gyri and in the adjacent part of the central insular sulcus (Figs. 3 and 4). In the representation of LE, these extremes are therefore the two insular fields differing most in terms of their respective connectivity patterns.

To evaluate the topographic distribution of the connectivity patterns from different insular territories, we masked all the regions on the cortical surface reached by probabilistic tractography in at least half of the participants (five subjects), and we color-matched each location on the surface with the insular location from which the largest amount of samples, averaged over all the subjects, were recorded during tractography (Fig. 4, bottom row). The cortical regions receiving most of the projections from the anterior insula included the OFC, pars orbitalis and several locations in pars triangularis of the IFG, and the dorsal part of the temporal pole. Further analyses (see below: Topographical and cytoarchitectonic specificity of connectivity patterns across insular territories) found the centromedial nucleus and laterobasal complex of the amygdala to be connected prevalently with the anterior insula and specifically with the most ventral and anterior insular territory around the limen. On the other hand, most of the tractography samples from the posterior dorsal insula reached the parietal lobe, including SI, SII, and the posterior parietal lobule as well as posterior regions of the temporal lobe in the superior temporal gyrus, the superior temporal sulcus, and the middle temporal gyrus. Samples from the insula, and especially from this posterior portion, were also recorded in extrastriate regions of the occipital cortex both medially (lingual gyrus) and laterally (putative BA19; about this see Discussion section: A comment on the claustrum). Regions in the frontal lobe that were mostly connected with the posterior dorsal insula included cortical territories in the premotor cortex, in pars triangularis and pars opercularis of the IFG as well as in the left dorsolateral prefrontal cortex (putative BA46). Middle insular territories displayed a mixed connectivity pattern between anterior and posterior insula. Cortical regions receiving the largest amount of samples from middle insular territories were located mostly in the lateral and medial premotorcortex as well as in regions of the temporal and parietal lobe adjacent to those reached by the posterior dorsal insula. Several territories in the IFG and OFC were also mostly reached by samples from the middle insula.

Gradual Versus Clustered Trajectory of Connectivity Variability

We analyzed the LE of the insula and of the mPMC to test the hypothesis of a smoother transition across connectivity patterns in the insula compared to a region like mPMC where previous studies found clusters of seed voxels featuring sharply different connectivity patterns. Wilcoxon signed rank test revealed that the size of the gaps along the trajectory of connectivity variability defined by the LE was significantly higher for the mPMC than for the insula in both hemispheres, suggesting the presence of comparatively sharper clusters in the examined medial frontal ROI with respect to the insula: right mPMC median gap = 0.0198, right insula median gap = 0.0125: $W_{\mathrm{mPMC}} =$

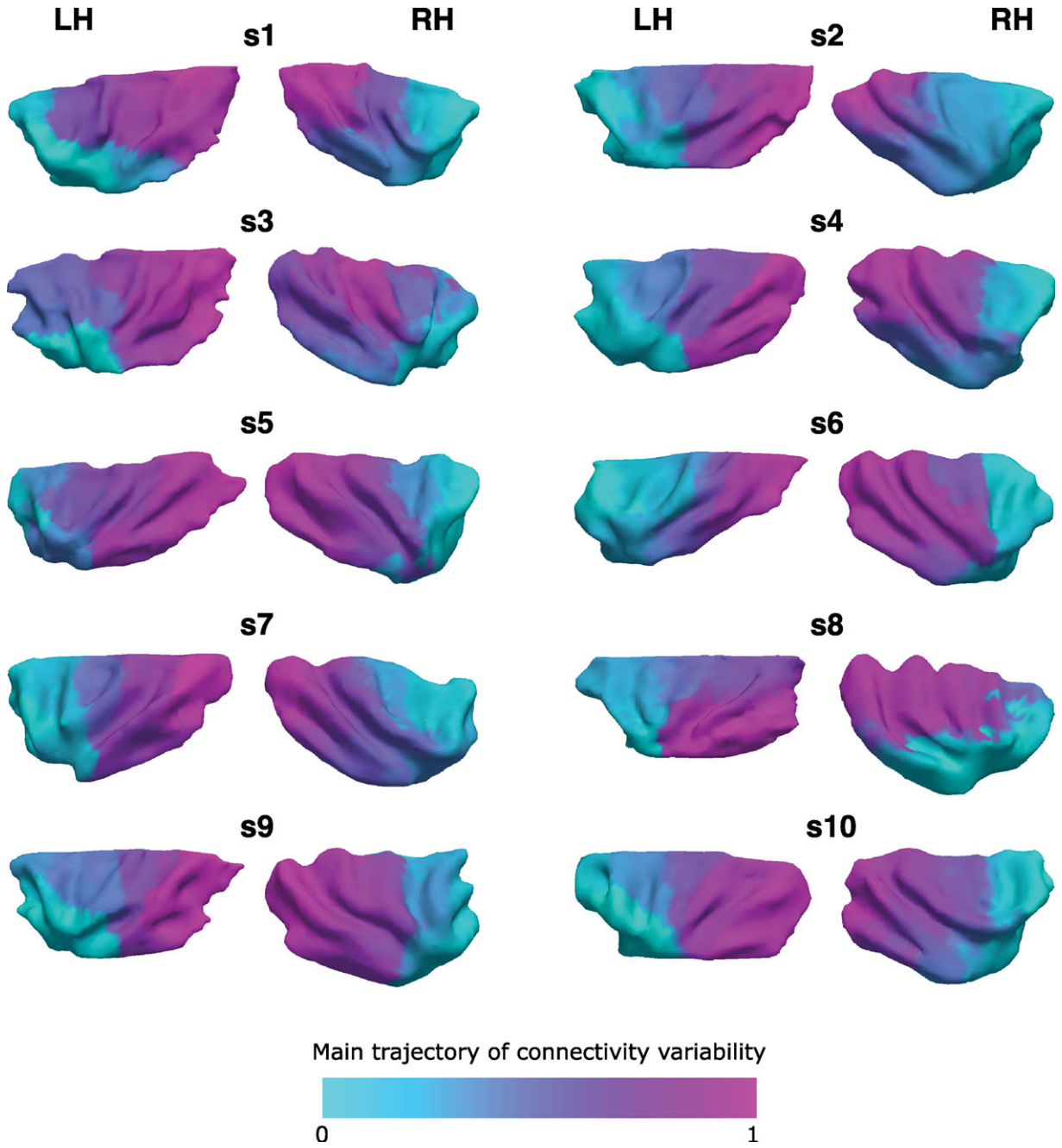

Figure 3.

Laplacian eigenmaps of the insula for each subject: Laplacian eigenmaps of the connectivity feature vectors derived from the in vivo probabilistic tractography in each subject and hemisphere. For purposes of visualization, Caret (http://www.nitrc.org/projects/caret/) was used to segment gray and white matter and produce fiducial surface representation [Van Essen, 2005] of the insula at approximately mid-way through the cortical gray matter (cortical layer 4) [Van Essen et al., 2001]. The final images of the surfaces and the mapping of the metrics derived from the Laplacian eigenmaps were rendered by means of Paraview (http://www.paraview.org/). Values on the surface were mapped from the volume containing the results of Laplacian eigenmaps and quantifying the distance along the main trajectory of connectivity variability: each vertex on the surface was assigned the value of the closest voxel in the volume. [Color figure can be viewed in the online issue, which is available at wileyonlinelibrary.com.]

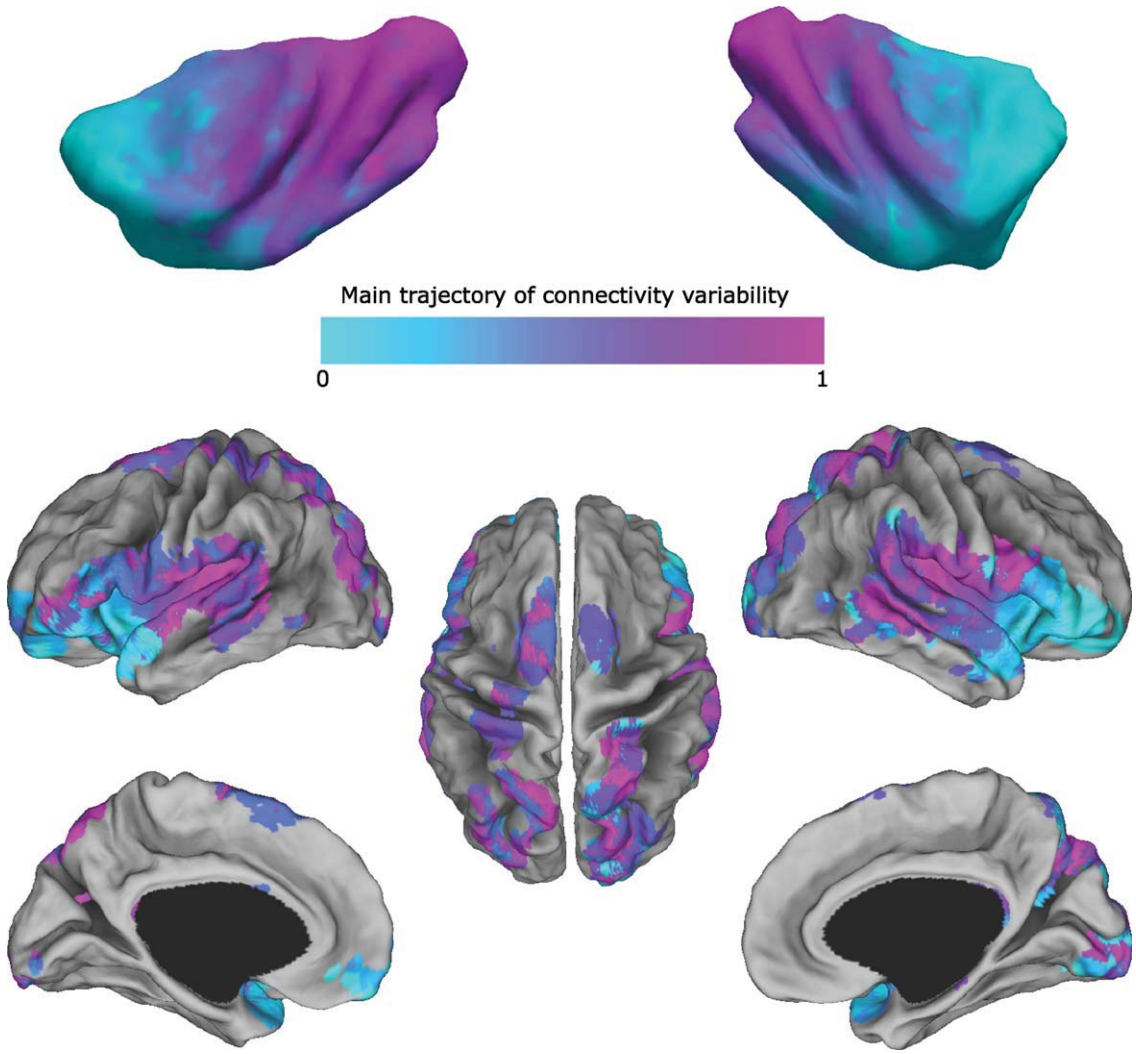

Figure 4.

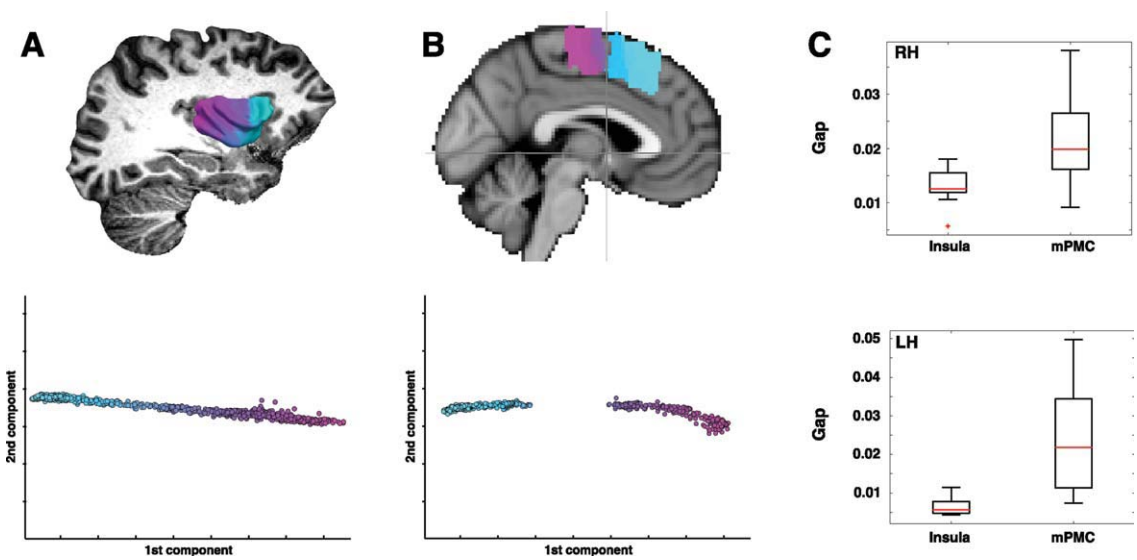

Figure 5.

138, $Z = 2.46$, $P < 0.014$.; left mPMC median gap = 0.0218, left insula median gap = 0.0057: $W_{mPMC} = 149$, $Z = 3.29$, and $P < 0.0011$ (see Fig. 5).

Topographical and Cytoarchitectonic Specificity of Connectivity Patterns Across Insular Territories and Between Hemispheres

Tracer-injection studies in macaques evidenced a topographic similarity between the trajectory of variation in the cytoarchitecture, organized radially around the ventral anterior agranular insula, and the trajectory of variation of insular projections, organized along a rostrocaudal axis [Chikama et al., 1997; Mesulam and Mufson, 1982b]). The rostrocaudal gradient of connectivity variability recovered in our study with LE was therefore expected to reflect changes in the connection probability with regions featuring different cortical types. To assess this hypothesis, we used 7 MPM of cytoarchitectonically defined regions in the atlas of Juelich [Eickhoff et al., 2005b] spanning a wide spectrum of cortical types ranging from agranular (amygdala, hippocampus, EC, and BA6) to dysgranular (BA44) to granular cortex (BA45, SI, SPL, and IPL), and we quantified the connection probability, averaged across subjects, of each voxel in the insula with each MPM. For example, the connection probability of a voxel in the insula with BA44 is quantified as the number of samples from that voxel reaching BA44, divided by the total number of samples reaching all the seven explored target regions. This measures the *selectivity* of the connections from insular voxels to targets, rather than the absolute number of samples (the latter was quantified previously, and shown in Fig. 4). Results of this analysis are shown in Figure 6A, overlaid onto the insular surfaces of the single-subject MNI template.

The connection probability maps show that some insular territories are characterized by relatively exclusive connections with specific targets, while others send a comparable number of seeds to all examined targets. In particular, the

Figure 4.

Average trajectory of connectivity variability and maximum number of tractography samples per target voxels. Average trajectory of connectivity variability (upper row): For visualization purposes, after calculating the Laplacian eigenmaps of the insular connectivity for each subject and each hemisphere, and replotting them into each subject's anatomical space, the volumes were transformed into the standard MNI space (see details in Methods section: Laplacian eigenmaps of the insula), and the median value for each insular voxel belonging to at least half of the participants was calculated and mapped onto the insular surface of the MNI single subject template [Holmes et al., 1998]. This illustration serves to show the rostrocaudal topographical arrangement of the recovered trajectory of connectivity variability, spanning from the most anterior insular territory, in the anterior short gyrus and in the ventral anterior insula around the limen, to the posterior insular territory, in the dorsal caudal long gyri and adjacent central insular sulcus. The same trajectory of variability was recovered in all subjects, as it can be appreciated from Figure 3. Additional analyses, comparing the single subject's Laplacian eigenmaps of insula and medial premotor cortex, were performed to test for the gradual versus clustered organization of connectivity patterns (see Methods and Results sections: Gradual versus clustered trajectory of connection variability; Discussion section: Gradual variation of connectivity patterns). Maximum number of tractography samples per target voxels (lower row): We thresholded the single subject's connectivity map for each seed voxel to a minimum of 50 samples, and we considered only target brain voxels reached in at least half of the participants (five subjects). Then, we color-matched each of the surviving target brain voxels with the insular location, derived from the average trajectory of connectivity map, from which it received the maximum number of samples, averaged over all subjects present in that location. [Color figure can be viewed in the online issue, which is available at wileyonlinelibrary.com.]

Figure 5.

Comparison between insula and medial premotor cortex. **A**: Laplacian eigenmaps identified the main trajectory of connectivity variability in the insula along the rostrocaudal axis. The absence of large gaps in the Laplacian eigenmap suggests the presence of a smooth transition across different connectivity patterns. **B**: On the other hand, the medial premotor cortex (mPMC) features a sharp transition between clusters with different connectivity patterns, which are evidenced by the presence of large gaps in the corresponding Laplacian eigenmap. The Laplacian eigenmap of the mPMC is overlaid onto the MNI single subject template to show that the transition is located on the plane through the anterior commissure (indicated by the cross-hairs). The size of the largest gaps in the Laplacian eigenmaps of insula and mPMC was therefore taken as a measure of the presence of sharp transition in connectivity patterns and compared between the two seed regions across all subjects. **C**: Boxplots (median, interquartile range, and most extreme values within 1.5 times the interquartile range) of the maximum detected gap in the Laplacian eigenmaps of insula and mPMC in both hemispheres. Wilcoxon signed-rank test showed a significant difference between the medians of the maximum detected gap in the insula and the mPMC. [Color figure can be viewed in the online issue, which is available at wileyonlinelibrary.com.]

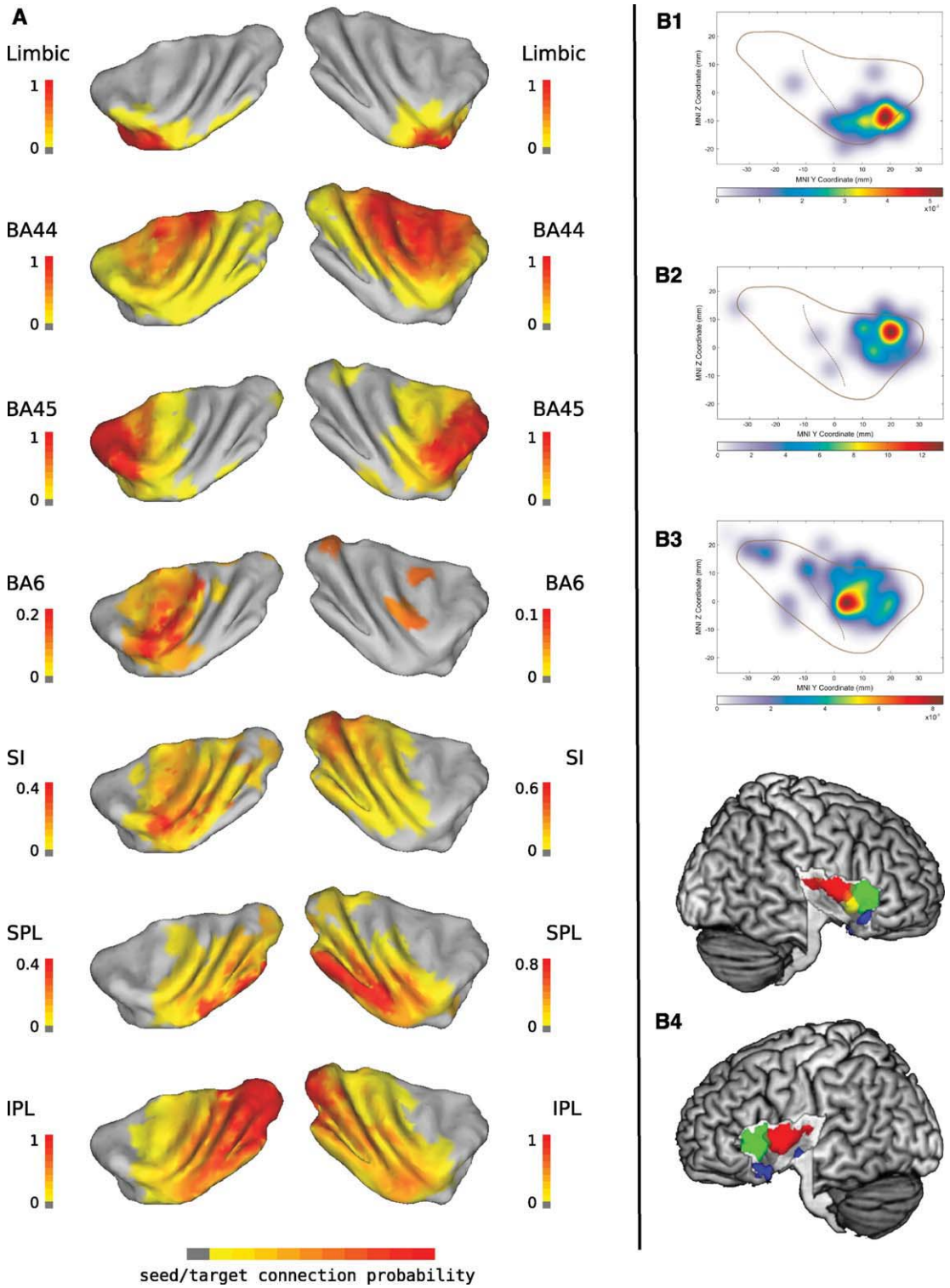
A
Limbic
1
0
Limbic
1
0
BA44
1
0
BA44
1
0
BA45
1
0
BA45
1
0
BA6
0.2
0
BA6
0.1
0
SI
0.4
0
SI
0.6
0
SPL
0.4
0
SPL
0.8
0
IPL
1
0
IPL
1
0
seed/target connection probability
B1
MNI Z Coordinate (mm)
MNI Y Coordinate (mm)
B2
MNI Z Coordinate (mm)
MNI Y Coordinate (mm)
B3
MNI Z Coordinate (mm)
MNI Y Coordinate (mm)
B4

Figure 6.

ventralmost anterior insula around the limen, location of the putative agranular insula, sends the vast majority of its samples to the limbic ROI, the dorsal anterior insula to BA45, and the caudal portion of the long insular gyri to the posterior parietal lobule. The middle insula, on the other hand, sends comparable amounts of samples to all but the limbic target.

When comparing the number of samples sent from the insular cortex to each of the examined targets in the RH and LH hemisphere, we found significant differences in BA44 (RH > LH, $t = 4.33$, $P < 0.002$) and SPL (RH > LH, $t = 3.24$, $P < 0.011$). On the other hand, the extent of insular cortex found to be connected to each target significantly differed for the Limbic target (LH > RH, $t = 3.41$, $P < 0.0077$) and for BA6 (LH > RH, $t = 2.543$, $P < 0.032$; Supporting Information Fig. S3). The latter result was also reflected in the maps showing for each insular voxel the number of subjects with an above-threshold number of samples to that target (Fig. 7, up). It is noteworthy the fact that in these two regions as well as in SI, there is a considerable spread of the centers of gravity of the connected insular region in the right hemisphere, suggesting a degree of variability across subjects in the extent of the connected insular cortex, even though the amount of samples sent to the respective target turned out to be comparable. However, we note that no significant difference was found when comparing between the two hemispheres, and for each target region, the variability in the distance of every subject's COG from the mean COG (Levene test: all $P > 0.184$; Brown–Forsythe test: all $P > 0.174$). Finally, in the case of SI, IPL, and left BA45, Figure 7 (up) suggests that across subjects, a consistent amount of tractography samples were sent from two spatially different insular territories.

DISCUSSION

We examined the anatomical distribution of insular connections in humans by means of in vivo probabilistic tractography in order to compare the results with the evidence from tracer-injection studies in macaques. LE on the results of probabilistic tractography showed that the main trajectory of connectivity variation in the human insula is organized along the rostrocaudal axis. The subsequent connectivity-based classification analysis suggested a relationship between the topographical variation of connectivity patterns and the variation of cytoarchitecture, similar to what has been found in macaques. The comparison between the LE of insula and mPMC suggests that the regional transition among different tractography patterns in the insula is smoother than in other brain regions.

In the following, we will first discuss these main findings. Also, because patterns of anatomical connectivity are important indicators of the functionality of different brain regions, we will discuss our results in comparison with recent findings about the involvement of the insula in speech production and in the experience of pain. In the speech domain, we will assess the specificity of projections from the anterior insular cortex to brain regions involved in speech production. In the pain domain, we will compare the locations in the insula where a prevalence of either limbic or somatosensory connections was found by probabilistic tractography, with the location of insular territories specialized for different aspects of the pain experience. Finally, we will discuss our results in relation with the findings from recent meta-analyses on the functional organization of the insula [Kurth et al., 2010b; Mutschler et al., 2009], and we will review two recent parcellation studies

Figure 6.

Connection probability maps with cytoarchitectonically defined regions and results from previous fMRI meta-analyses. **A**: Average (median) connection probability for each insular voxel present in at least half of the participants (five subjects), calculated for the maximum probability maps (MPM) of several cytoarchitectonically defined regions in the atlas of Juelich [Eickhoff et al., 2005b]. The values are plotted on the insular surface of the MNI single subject template. The Limbic ROI (amygdala, EC, and hippocampus), BA44, BA45, BA6, primary somatosensory cortex (SI), superior (SPL), and inferior (IPL) parietal lobule MPMs were chosen to evaluate the different connection probability of different insular territories because of their known connectivity with the insula from animal studies as well as for the wide range of cortical types that they span. The anterior ventral insula, putative location of the agranular insula, had the highest connection probability with the limbic ROI, while the highest connection probability with posterior parietal regions was found in the posterior gyri of the insula, putative location of the granular, and adjacent dysgranular insula. These two regions featured the two extremes of the trajectory of connection probability found with Laplacian eigenmaps (see Figs. 3 and 4). **B1–B3**: Maps showing the results of the meta-analysis of the functional organization of the anterior insula performed by Mutschler et al. ([2009]—reproduced with permission of Elsevier) on 58 fMRI studies, reporting in total 159 peaks of activation. B1 refers to studies related to peripheral and autonomic changes as well as co-activation of voxels in the insula and in the amygdala; B2 refers to studies on auditory and language processing; B3 refers to studies involving hand movements. **B4**: Result of the meta-analysis performed by [Kurth et al., 2010] on coordinates from 1768 studies retrieved from the BrainMap database [Fox et al., 2005a; Laird et al., 2005, 2009] and Pubmed. In the result shown here (adapted from Fig. 7 in Kurth et al. [2010] and reprinted with permission of Springer), studies from 13 functional categories were grouped in four domains to investigate the presence of domain-specific functional specialization in the entire insular cortex: sensorimotor (red), cognitive (green), chemical sensory (yellow), and social emotional (blue). [Color figure can be viewed in the online issue, which is available at wileyonlinelibrary.com.]

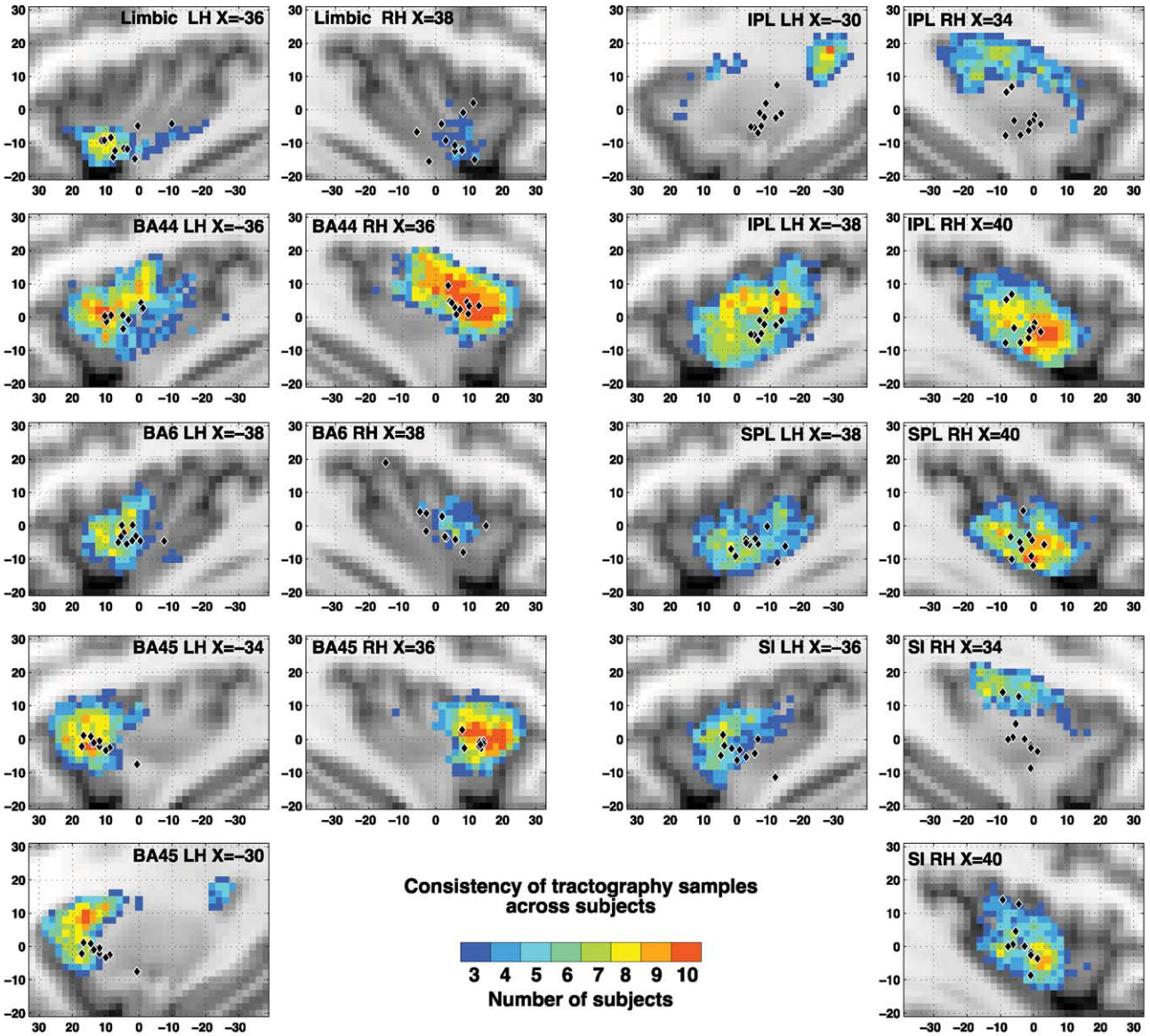
Limbic LH X=-36
Limbic RH X=38
IPL LH X=-30
IPL RH X=34
BA44 LH X=-36
BA44 RH X=36
IPL LH X=-38
IPL RH X=40
BA6 LH X=-38
BA6 RH X=38
SPL LH X=-38
SPL RH X=40
BA45 LH X=-34
BA45 RH X=36
SI LH X=-36
SI RH X=34
BA45 LH X=-30
SI RH X=40
Consistency of tractography samples across subjects
3 4 5 6 7 8 9 10
Number of subjects

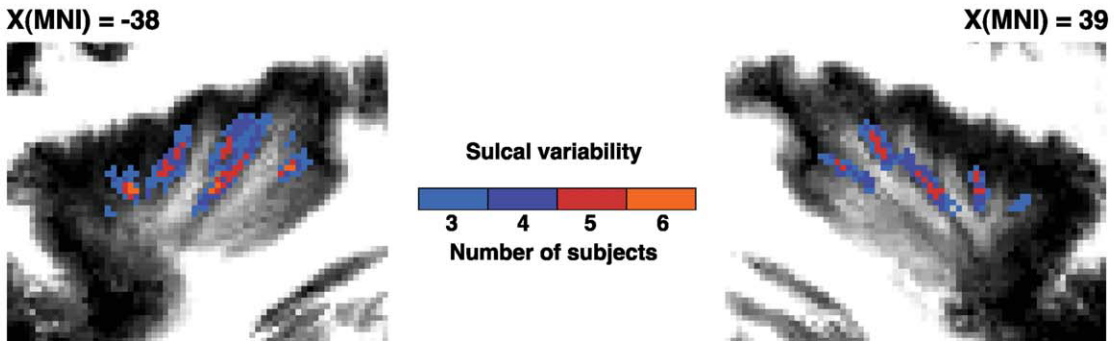
X(MNI) = -38
X(MNI) = 39
Sulcal variability
3 4 5 6
Number of subjects

Figure 7.

on the insula based on resting-state functional connectivity [Cauda et al., 2011; Deen et al., 2010].

Trajectory of Connectivity Variability in the Insular Cortex

Our results are in line with the evidence from tracer-injection studies in macaques in several respects. First, LE revealed a relatively smooth transition across connectivity patterns, topographically arranged along the rostrocaudal anatomical axis. Several cytoarchitectonic studies in macaques explicitly report that a gradual transition across cortical types [Friedman et al., 1986; Jones and Burton, 1976; Mesulam and Mufson, 1982a, 1985], as well as in the amount of intracortical myelin [Friedman et al., 1986; Mesulam and Mufson, 1982a], is reflected in the transition among different connectivity patterns [Chikama et al., 1997; Mesulam and Mufson, 1982b, 1985]. Also, tracer-injection studies in macaques suggested the presence of a gradual change in the insular connections with the amygdala [Amaral and Price, 1984], the striatum [Chikama et al., 1997; Fudge et al., 2005] and the secondary somatosensory cortex [Friedman et al., 1986].

Second, the comparison between the topographical arrangement of seed and target voxels suggests the presence in humans of a relationship between the variation of the cortical types and the variation in the anatomical connections as previously found in macaques. Tracer-injection studies evidenced that the Ia and Ig have very different connectivity, often with brain regions featuring the same cytoarchitecture [Amaral and Price, 1984; Augustine, 1985, 1996 for a review; Fudge et al., 2005; Mesulam and Mufson, 1985; Mufson and Mesulam, 1982]. In our study, as we matched each location on the cortical surface, reached by probabilistic tractography in at least half of the participants, with the insular territories from which they received the maximum projections, we observed that the OFC, the anterior parts of the IFG as well as the amygdaloid complex were mostly reached by samples from the connectivity distribution of the anterior insular territory encompassing the ventral anterior insula around the limen and the anterior short gyrus, where the Ia and the adjacent Id were, respectively, located in previous histological studies [Bonthius et al., 2005; Mesulam and Mufson, 1982a; Ongur et al., 2003]. On the other hand, parietal and posterior temporal regions, several locations in the lateral premotor cortex, and in posterior territories of the IFG were mostly reached by samples from the posterior insular territory encompassing the dorsal part of the long insular gyri and the adjacent central insular sulcus, in the location of Ig and adjacent Id [Bonthius et al., 2005; Kurth et al., 2010a; Mesulam and Mufson, 1982a].

Third, in macaques, the dysgranular insula projects to brain regions ranging from allocortex to homotypical isocortex [Amaral and Price, 1984; Augustine, 1985, 1996 for a review; Fudge et al., 2005; Mesulam and Mufson, 1985; Mufson and Mesulam, 1982], and different territories of Id display different connectivity patterns according to the proximity with either Ia or Ig [Mesulam and Mufson, 1985]. In our study, we found that territories lying in the middle insula displayed a wide spectrum of connections including cortical regions in the parietal and temporal lobe, the whole IFG, and scattered locations in the OFC as well as widespread connections to the premotor cortex. The anterior extreme of the connectivity variability encompassed the putative locations of both Ia and adjacent Id, which were found to have very similar connectivity patterns in macaques (see Fig. 9 in Mesulam and Mufson [1982b]), while samples from more caudal insular territories, in the putative posterior Id, were mostly found in regions of the cortical surface adjacent to those reached by the other extreme of connectivity variability in the most dorsal and caudal insula.

Comparison with Evidence from Studies in Macaques

A relationship between connectivity and cytoarchitectonic variation was also suggested by the analysis of the insular connection probability to 7 MPM taken from the probabilistic cytoarchitectonic atlas of Juelich [Eickhoff et al., 2005b] and chosen among the available maps in

Figure 7.

Lateralization and consistency maps. Up: Consistency maps showing for each insular voxel the amount of subjects which showed an above-threshold amount of tractography samples to each of the seven examined targets: Limbic ROI (amygdala, enthorinal cortex, and hippocampus), BA44, BA45, and BA6, primary somatosensory cortex (SI), superior (SPL), and inferior (IPL) parietal lobule. The parasagittal slice showed here was chosen to display the coordinate corresponding to the maximum overlap across subjects. For clarity, only voxels with three or more overlapping subjects are displayed. In the case of SI, IPL, and BA45, consistent projections across subjects were found in two spatially different insular territories (in one or both hemispheres). Black diamonds indicate the locations of the center of gravity (COG) of the connected cluster in different subjects. Down: Sulcal variability map. After registration of each-subject skull-stripped anatomical (T1-weighted) image to the MNI single subject template [Holmes et al., 1998], sulcal outlines were drawn manually on two single sagittal slices. The consistency map of the location of the sulci across is presented here overlaid onto the average anatomy across all the participants. The outline of each subject's sulci can be seen in Supporting Information Figure S4. [Color figure can be viewed in the online issue, which is available at wileyonlinelibrary.com.]

order to include regions known to be connected with the insula and to span a wide spectrum of cortical types: BA44, BA45, BA6, SI, inferior and superior parietal lobule, and a limbic ROI, encompassing amygdala, EC, and hippocampus. The limbic ROI had the strongest connection probability to the anterior ventral insula, while SI and IPL had the strongest probability of connection with the posterior dorsal insula. Territories in the putative Id shared similar connection probability with all the examined maps and were also the target of the maximum connection probability for BA44, BA6, and BA45.

The topographic arrangement of connection probabilities in the insular cortex with these regions was also mostly consistent with studies in macaques and will be considered separately in what follows.

Limbic connectivity

Anatomical studies have consistently found that the insular cortex has extensive limbic and paralimbic connections concentrated mostly in its anteroventral territories (see Augustine [1985] and Mesulam and Mufson [1985] for a review), which have themselves been included in the definition of the limbic lobe [Heimer and Van Hoesen, 2006; Morgane and Mokler, 2006]. To quantify insular connectivity with other structures of the limbic system, we used a cytoarchitectonically defined ROI encompassing amygdala, EC, and hippocampus [Amunts et al., 2005]. We found the highest probability of connection with these regions in the most rostral ventral insular field, corresponding to the putative agranular insula, in line with animal findings [Aggleton et al., 1980; Amaral and Price, 1984; Kerr et al., 2007; Mohedano-Moriano et al., 2007; Mufson et al., 1981; Stefanacci and Amaral, 2002].

IFG and premotor cortex

Comparing the projections to the inferior frontal gyrus (IFG) and adjacent ventral premotor cortex in our study with evidence from animal studies is complicated by the lack of a definitive agreement regarding the homologies between the subdivisions of this region in macaques and humans [Gerbella et al., 2007; Geyer et al., 2000; Petrides and Pandya, 2002; Petrides, 2005; Rizzolatti et al., 1998]. Although the exact border separating the macaque homologues of human BA45, 44, and 6 remains disputed, a certain consensus is emerging: the anterior bank of the inferior ramus of the arcuate sulcus and the adjacent rostral convexity are thought to be homologous to human BA45, while its posterior bank and adjacent caudal convexity fall within the homologues to human BA44 and lateral BA6 [Belmalih et al., 2007; Brodmann, 1909; Geyer et al., 2000; Matelli et al., 1985; Nelissen et al., 2005; Petrides, 2005; Rizzolatti and Arbib, 1998; Vogt and Vogt, 1919].

BA44 and ventral BA6. Mesulam and Mufson [1982b] and Mufson and Mesulam [1982] found the caudal bank of the ventral arcuate sulcus to be connected with the middle insula. Matelli et al. [Matelli et al., 1986] replicated these results, also finding the caudal convexity to be connected with the middle insula, but in the latter study, the staining extended slightly more rostrally in the dysgranular insular territory. Consistent with these evidences, we found that BA44 and ventral BA6 had their maximum connection probability to the dorsal part of the middle insula in the territory of the middle and posterior short gyri (see Fig. 6). We also note that most of the projections to ventral BA6 originated from the middle insula (see Fig. 4).

BA45. Previous studies showed evidence for moderate anatomical connections between dysgranular and granular insula and the macaque homologue of BA45 [Gerbella et al., 2010; Mesulam and Mufson, 1982b; Petrides, 2006; Petrides and Pandya, 2002]. In agreement with these findings, Figure 4 shows that sectors of the left BA45 receive most of the tractography samples from territories in the middle and posterior insula. We also observed that the anterior dorsal insula (Fig. 6A), found to be involved in language processing (see Fig. 6B2 and Discussion: Comparison with functional studies), sends more samples to BA45 than to the other six ROIs we considered for quantifying connection probability. This latter finding should however be considered in the light of the fact that more posterior territories of the insula total substantially more samples to BA45 than this anterior region (Fig. 4 and Supporting Information Fig. S1).

Dorsal and medial BA6. In macaques, the posterior insula was shown to be connected with both F3 and F6 on the medial wall, with the most consistent connections between the granular insula and F3 [Luppino et al., 1993]. In our study, we found tractography samples from the insula in the most dorsal extent of the premotor cortex as well as in the supplementary motor area (the human homologous of macaque area F3 [Picard and Strick, 1996]). The seed regions were mostly located in the putative posterior dysgranular and granular insula (see Fig. 4).

Primary somatosensory cortex

Tracer injection studies in macaques have shown that SI is strongly reciprocally connected with the insula and especially with posterior territories spanning the granular and adjacent dysgranular fields [Darian-Smith et al., 1993; Friedman et al., 1986; Mesulam and Mufson, 1982b]. Also, a large portion of Ig was shown to be modality-specific for tactile stimuli [Schneider et al., 1993]. Mesulam and Mufson [1985] indicated a bifocal projections to the face and leg/foot representation territories of SI in the dorsal Id and Ig, possibly underlying a somatotopic organization. We found a similar connectivity pattern with projections both to the foot and the dorsal crest of the anterior

postcentral gyrus, mostly originating in the middle and caudal insular cortex.

Inferior and superior parietal lobule

Several anatomical works in the last decade have consistently reported the presence of anatomical connections between the posterior parietal cortex and the insula, with projections to the IPL, and especially from its anterior portion, concentrated mainly in the granular insula and to a lesser extent in the adjacent dysgranular fields [Andersen et al., 1990; Cavada and Goldman-Rakic, 1989; Mesulam and Mufson, 1982b, 1985; Neal et al., 1987; Rozzi et al., 2006]. In our study, we found the posterior dorsal part of the insula, in the region of the long insular gyri, to have the maximum connection probability with IPL. The maximum connection probability with SPL, on the other side, was recorded in a region corresponding to the posterior long gyrus, in line with the observations from Mesulam and Mufson [1982b].

Differences between human and macaque insula

There are currently two strong sources of information about the connectivity of the human brain: (1) in vivo tractography studies of the human brain, with their technical shortcoming—that we discuss in the Conclusion section of this work—and (2) invasive tracer injection studies in the macaque brain, with their problems associated with differences between species. Although these two methods are each affected by their own shortcoming, the source of errors in the two methods is different and independent. We and others before us [Anwander et al., 2007; Beckmann et al., 2009; Croxson et al., 2005; Johansen-Berg et al., 2004, 2008; Klein et al., 2007; Tomassini et al., 2007] therefore seek to reduce the overall uncertainty by generating our hypotheses for tractography studies and validate our results using the evidence gathered from tracer injection studies in macaques. We therefore feel that combining two methods with independent problems, namely human tractography and macaque tracer studies, remains to date the best approach to shed light on human connectivity. Until more precise methods will be developed, which can deliver the same accuracy of tracer-injection studies, we can only highlight the current evidence suggesting actual differences across species, and reason about the possible implications for tractography results.

One difference between human and macaque insula regards the Von Economo neurons (VEN) [Nimchinsky et al., 1999; von Economo and Koskinas, 1925], which are present in the insula and in the anterior cingulate cortex (ACC) of humans and great apes, while they are absent in macaque. These neurons were found in humans especially in the agranular insula and gradually decreasing toward the superior anterior insula [Allman et al., 2010]. It has been hypothesized that these neurons could represent the substrate for fast relaying interoceptive, emotional, cognitive, and sensory information to other parts of the brain, particularly for the purpose of generating fast adequate response in fast-paced behaviours, such as during social interaction [Allman et al., 2010; Craig, 2009]. Indeed, these neurons are greatly reduced in pathological conditions presenting marked deficits in social cognition such as frontotemporal dementia [Seeley, 2010; Seeley et al., 2006] and agenesis of the corpus callosum [Kaufman et al., 2008]. Craig proposed that VENs could be involved in the fast interconnections between the anterior insula and the ACC [Craig, 2009]. A first result obtained with diffusion tensor tractography in a 27-year-old male gorilla indicated connectivity of the insular region containing VENs with the frontal pole, as well as other parts of frontal and insular cortex, the septum and the amygdala, and close examination of the reported images also suggests a connection with ACC [Allman et al., 2010]. Using very high-spatial resolution DW data (90 micra cubic voxels) on formaldehyde-fixed specimens, researchers from the same lab were able to reconstruct connectivity maps between the insula and ACC in mouse lemur, macaques, and gorillas (Park et al., personal communication). In a recent in vivo tractography study in humans, connections between the anterior insula and ACC have been reported [van den Heuvel et al., 2009]; however, in that study, the insular and ACC ROIs, identified by resting-state functional connectivity analysis, apparently extended to adjacent territories (in the opercula and in the medial motor wall, respectively—cfr. Fig. 6 in van den Heuvel et al. [2009]) and were also dilated to a maximum of 4 mm before performing tractography. Another study using probabilistic tractography and focusing on the connection of the entire cingulate cortex did not report any connections with the insula [Beckmann et al., 2009], and the same result was found in the present work. We believe that these diverging results are due to a limitation in the current methods in tracing fibers through major fiber bundles like the corona radiata and the corpus callosum, and more generally in regions of high structural complexity [Beckmann et al., 2009], as well as from the limitations of the quality of the DW data, which are currently obtainable with in vivo studies in humans. With respect to our study, because our hypothesis was derived from evidences in macaque, in which VENs appear not be present, it is legitimate to ask in which way this difference would affect the trajectory of connectivity variability in the insula. Preliminary tractography results from our lab suggest that LE recovers an analogous difference in the rate of change of connectivity patterns in humans and macaques when comparing insula and mPMC (see Supporting Information Fig. S2 and [Cerliani, 2009]). Nevertheless, current MR tractography techniques can only analyze the connectivity of large ensembles of neurons and axons and therefore cannot specifically examine the connectivity of VENs. Also, to our knowledge, the connectivity of VENs still needs to be analyzed by means of traditional tracer injection techniques [Allman et al., 2010]. Finally, the

connectivity between insula and ACC in humans needs to be clarified by further analyses, given the divergence of the results in the current literature. It is therefore premature at this stage to attempt to answer to the question of whether and how the presence of VENs in humans but not in macaque would have affected the trajectory of connectivity variability, which can be recovered with probabilistic tractography.

Another notable difference between the functional neuroanatomy of human and macaque insula was found by studying taste representation in the insula. In macaques, anterograde tracer injections have shown that the primary gustatory cortex is located in the most rostral part of the superior limiting sulcus and more precisely in a small granular region at the insular/opercular junction of the frontal lobe [Pritchard and Norgren, 2004; Pritchard et al., 1986; Small, 2010]. On the other side, several functional neuroimaging studies in humans (reviewed in Small et al. [1999]) showed that taste response is localized in other, more posterior regions of the insula/frontal operculum, and that the most anterior dorsal part of the insula may be involved in a more integrative activity in the context of feeding behaviour [Small, 2010; Veldhuizen et al., 2008]: in the context of taste studies, Jabbi and colleagues [Jabbi et al., 2007] showed that the anterior dorsal insula is involved in both experience of disgusting tastants and observation of disgusted facial expressions in others and that the different sensitivity of the participants to the feelings of others predicted the activity of the same insular region when observing both pleased and disgusted facial expressions of others. Rather than a caudal "shift" of the primary gustatory cortex in humans, Craig [2009, 2010] proposed that this cortical territory in the human dorsal anterior insula in may lack an obvious morphological homologue in the monkey. On the basis of the extensive evidence from the functional neuroimaging literature, it was shown that the human dorsal anterior insula has a crucial role in integrating salient information from all neural systems at the present instant, which suggests that in humans, "right and left anterior insulae are crucial components of a network that engenders human awareness" [Craig, 2010]. Although it is difficult on the basis of the current evidence to determine whether the anterior insula of humans represent a newly evolved structure, we mention that one allometric study [Semendeferi and Damasio, 2000] reported that the human insula may have increased more than expected during hominid evolution; however, the results did not reach significance, and the authors concluded that the amount of examined MR images ($N = 29$, 10 humans) was not large enough to be confident in the obtained results.

Suggested Asymmetries in the Tractography Results

Our tractography results suggested differences in the connectivity maps of the right (RH) and left (LH) insula. We therefore performed additional analyses to study interhemispheric differences in the tractography samples to the target regions chosen to perform connectivity-based classification, and we considered differences in the extent of the insula connected to each target, and the variability across subjects of the centers of gravity of the connected insular territory. To our knowledge, evidence of lateralization of insular connections in macaques is lacking; however, functional neuroimaging investigations in humans added valuable information about functional and structural asymmetries in the insula and provide in some cases arguments for a discussion of our tractography findings. Watkins et al. [2001] analyzed 142 healthy adults with voxel-based morphometry and found RH $>$ LH asymmetry in the amount of gray matter in the anterior inferior insula. In a study on 300 MRI images and 16 fixated brain specimen, Naidich et al. [2004] documented the variability in the configuration of insular gyri as well as differences in this configuration between LH and RH insulae, often in the same subject. A recent meta-analysis on 1768 fMRI experiments suggests the presence of asymmetries in the insula for some functional categories such as taste, interoception, somatosensation, empathy, and speech [Kurth et al., 2010b]. On the basis of a great amount of evidence indicating a forebrain emotional asymmetry, Craig [2005, 2009, 2010] proposed that RH and LH anterior and mid insula are associated with sympathetic and parasympathetic activity, respectively, and that their coordinated activity embodies a neural system aimed at optimizing energy expenditure. Finally, we mention that a recent work used metrics from graph theory on whole-brain tractography and found a RH $>$ LH asymmetry for measures of global efficiency and interconnectivity, as well as for regional measures of betweenness centrality, or relative importance of several brain regions for the connectivity of the whole network [Iturria-Medina et al., 2011]. Results in the present work suggest on a global level that the RH anterior insula has a more widespread connectivity patterns with respect to the LH anterior insula (see Fig. 4). Although the results from Iturria-Medina and colleagues did not find significant difference of betweenness centrality for the RH or LH insulae, we suggest the possibility that such difference could be found by comparing only the anterior insulae.

The insular region sending above-threshold samples to the Limbic ROI was found to be significantly bigger in the LH, even though the difference in the number of samples recorder in the Limbic ROI did not significantly differ between hemispheres. It is possible that the detection of connectivity with the limbic lobe was favoured in the LH by a reported leftward asymmetry of fractional anisotropy (LH $>$ RH) of the subinsular portion of the uncinate fasciculus [Kubicki et al., 2002; Rodrigo et al., 2007]; on the other side, a completely different hypothesis points to the presence of a region in the mid-posterior ventral insula, consistent with the location our results (see Fig. 7) which was found in a recent meta-analysis to be specifically involved in empathy [Kurth et al., 2010b].

Samples to the primary somatosensory cortex (SI) were sent from the middle insula in both hemisphere; however, the RH insula was characterized by a second territory of consistent projections across subjects, located in the posterior insula. An interesting hypothesis is that this asymmetry is related to the extensively described RH posterior insula involvement in the sense of limb ownership in both healthy subjects and patients (see Ibanez et al. [2010] and Karnath and Baier [2010] for reviews). Several clinical studies [Baier and Karnath, 2008; Cereda et al., 2002; Karnath et al., 2005] reported that in patients with hemiparesis/hemiplegia, the presence of anosognosia and other "disturbed sensation of limb ownership" (DSO [Baier and Karnath, 2008]) is more frequent in cases of damages to the RH posterior insula. In healthy subjects, the rubber hand illusion paradigm was used to manipulate the sense of limb ownership by Tsakiris et al. [2007]. In this PET experiment, participants saw either a right or a left hand being rubbed, in or out of synchrony with their own hidden right hand; they had to indicate the position of their limb before and after the stimulation. A correlation was observed between brain activity and the proprioceptive drift toward the rubber hand, in a region of the posterior RH insula that co-localizes with the area of maximum overlap in the posterior RH insular cluster found to be connected to SI (see Fig. 4A in Tsakiris et al. [2007]).

Several insights regarding the hemispheric asymmetry of insular connectivity with BA44 come from the extensive functional neuroimaging literature on the lateralized involvement of the insula in tasks related to speech and singing. For example, in the speech domain, the RH fronto-opercular region is involved in extracting slow pitch information from the speech stream, while the LH fronto-opercular region performs extraction of segmental units from the speech signal [Meyer et al., 2002; Wildgruber et al., 2004]. This evidence is strikingly in line with the observation that LH insular activity increases and the RH insular activity decreases, as a function of the rate of stimuli presentation (trains of clicks and syllables) [Ackermann and Riecker, 2004; Ackermann et al., 2001]. A lateralization effect is also suggested from experiments on the different meaning conveyed by prosody during speech production: while production of linguistic prosody (e.g., formulating a question) is associated with activity in the bilateral IFG and the LH insula, emotional prosody (e.g., a happy intonation) is associated with activity in the left IFG and in the RH insula [Aziz-Zadeh et al., 2010]. Finally, in a task involving either overt recitation of the months of the year or overt singing a nonlyrical tune, Riecker reported the same asymmetry for both insula and IFG: LH activity in these regions was associated with the speech production task, while RH activity was associated with the singing task [Riecker et al., 2000]. Given these evidence, and considering in general the role of the insula in dynamically integrating salient aspects of inner and outer environment to generate appropriate energy-efficient behavioral responses [Craig, 2009; Mesulam and Mufson, 1985], we suggest that the stronger connectivity between BA44 and RH insula found in our tractography study would make the right hemisphere better suited to convey the emotional state of the organism during speech production [Ackermann and Riecker, 2004] and, in general, during social interaction as well as during singing. Also, the RH insula could be particularly well suited for the on-line integration of somatosensory, kinesthetic, and auditory feedbacks, which is required for the enhanced vocal motor control during singing [Kleber et al., 2010].

Intersubjective Variability

In the present study, we also considered the intersubjective variability in the connection probability of the insula with several brain regions. We reported, for each target mask and hemisphere, spatial variability maps of the COG of the connected insular cluster across subjects (Fig. 7, up), quantified the spatial spread as a function of hemisphere and target, and computed consistency maps showing for each target mask how many subjects sent an above-threshold number of samples from each insular voxel (Fig. 7, up). This analysis suggested a considerable spatial variability, particularly in the right hemisphere, both in the COG and in the location of the insular voxels found to be connected with BA6, SI, and the Limbic ROI. Regarding the connectivity between insula and Limbic ROI, which was observed especially in the ventralmost anterior insula, we point out that this region is characterized by the presence of the transverse insular gyrus (TG). This region extends from the insular pole and apex to the posteromedial orbital lobule [Naidich et al., 2004; Ture et al., 1999] (see Fig. 2 in Naidich et al. [2004]) and represents the location where the densest concentration of VEN in the insula was found in humans (see Allman et al. [2010]; Fig. 3). Because this region is phylogenetically young [Rose, 1928], Craig [2010] proposed that large interindividual structural differences might be observed in the TG, and various dissection studies indeed reported considerable morphological variability in this region [Naidich et al., 2004; Ture et al., 1999; Varnavas and Grand, 1999].

Various studies on postmortem specimens and MR images reported a considerable variability in the sulcal and gyral morphology of the insular cortex in humans [Afif and Mertens, 2010; Johnson et al., 2009; Naidich et al., 2004; Ture et al., 1999; Varnavas and Grand, 1999] as well as across species [Butti and Hof, 2010]. The intersubjective variability in the spatial distribution of different cortical types was reported in a recent cytoarchitectonic parcellation study on the postcentral insular region [Kurth et al., 2010a]; however, in that study, the relationship between cytoarchitecture and sulcal variability was not examined. Intersubjective variability in sulcal morphology represents a well-known problem for group analyses in neuroimaging, because a misregistration of the sulci across subjects contributes to increase the probability of

performing group analyses on nonhomologous brain regions. Fully aware of these issues, when comparing the relative rate of change of the connectivity patterns in the insula and in the mPMC, we calculated the relevant measurements in each subject, hemisphere, and region of interest separately. The metric of interest was represented by the magnitude of the gaps in each subject's LE, with larger gaps denoting a more abrupt transition between connectivity patterns. By comparing the LE of insula and mPMC of each subject, Wilcoxson signed rank test reported significantly larger gaps in the LE of the mPMC, suggesting that the transition between different connectivity patterns is more gradual in the insula than in the mPMC. Because the gaps are calculated in the LE of each subject, hemisphere, and region of interest separately, rather than on a group average, the recovered difference in the rate of change of connectivity patterns cannot be affected by issues due to averaging across subjects, such as smoothing or misregistration across different brains. Regarding the issue of sulcal variability, we note that this analysis compares the magnitude of the gaps in the space of the LE of each single subject, independently of the anatomical location of those gaps, and therefore is not affected by intersubjective differences in sulcal morphology.

In this work, we report maps of sulcal variability in our sample (see Fig. 7, down), although here we do not investigate the link between the differences in the localization of the trajectories of connectivity variability and macroanatomical landmarks such as sulcal patterns. In which way, the morphological variability of the insula relates to cytoarchitecture, and functional difference is an important topic for future multimodal imaging studies. We note however that the available literature about humans do not reflect a general consensus regarding the relationship between cytoarchitecture and the sulcal anatomy (see also Supporting Information Fig. S5). In 1909, Brodmann divided the insula in two main cortical fields and stressed that their border, although in continuation with the central (Rolandic) sulcus, did not correspond exactly with the central insular sulcus [Brodmann, 1909; 122). The parcellation presented by Rose [1928] also displays some relationships with the sulcal morphology, although in some cases, and specifically in the middle and posterior short gyri, different cortical types are present. Even more complex is the scheme presented by Brockhaus [1940], in which the differentiation between the main cortical types is almost orthogonal with respect to the sulcal morphology. Similarly, the study performed by Bonthius et al. [2005] is in line with the report of Mesulam and Mufson [1982a] about the radial organization of the cytoarchitecture. Finally, the recent parcellation study by Kurth et al. [2010a] on the postcentral insular cortex maps the granular territories of the insula (Ig1 and Ig2) in the dorsal part of the postcentral gyri, caudally located with respect to the central sulcus as well as a dysgranular sector (Id1) located mainly in the posterior part of the IPS. The latter study is particularly important in the context of clarifying the relationship between sulci and cytoarchitecture, because it is the first observer-independent parcellation study of the insula. Maps of the anterior sector of the insula obtained with this methodology will help clarify whether a stronger consistency between cortical types and sulcal morphology can be recovered in the precentral insular territories.

A Comment on the Claustrum

The gray matter of the claustrum is located underneath the insular cortex. Middle and dorsal insular territories are separated from the claustrum by the extreme capsule, while the inner stratum of the agranular insula is coextensive with the claustrum [Bonthius et al., 2005; Mesulam and Mufson, 1982a]. Given the close proximity of insula and claustrum, and the spatial resolution of the acquired DW images, it is possible that some claustral gray matter was included in the ventral part of the insular ROI used to perform probabilistic tractography. One effect of this inclusion could have been the presence of samples located in extrastriate regions of the occipital lobe (lingual gyrus and lateral putative BA19), because, to our knowledge, no direct connections between the insula and the occipital lobe have been reported in animal studies. On the other hand, animal studies have shown the direct involvement of the claustrum in processing visual stimuli (see references in Crick and Koch [2005], Mufson and Mesulam [1982], Tanne-Gariepy et al. [2002]) as well as claustral connectivity with parieto-occipital regions [LeVay and Sherk, 1981; Shipp et al., 1998]. Moreover, a recent combined dissection and DTI study on the claustrum in humans [Fernandez-Miranda et al., 2008] suggested the existence of white-matter pathways between the claustrum and the occipital lobe via the inferior fronto-occipital fasciculus proposed by Catani et al. [2002] (but see a discussion on the existence of this fiber bundle in Schmahmann and Pandya [2007] and Schmahmann et al. [2007]).

If this partial volume effect would have had a major influence on the recovered structure of connectivity variability, our results should have displayed some consistency with the available knowledge from animal studies about the patterns of histological, functional, and/or connectivity variation in the claustrum that are known to differ from those in the insula [Brand, 1981; Kowianski et al., 1999; Mufson and Mesulam, 1982]. In contrast to the insula, whose connectivity is organized mainly along a rostrocaudal gradient [Mesulam and Mufson, 1982b] with its various territories showing comparatively distinct connectivity patterns, the claustrum is divided histologically [Brand, 1981] and morphometrically [Kowianski et al., 1999] in a dorsal and a ventral section, with comparatively unspecific projection to different cortical regions [Crick and Koch, 2005; Tanne-Gariepy et al., 2002]. It is therefore reasonable to conclude that the effect of potentially including part of the claustrum in our seed region must have had at most a minor effect on our results.

Gradual Variation of Connectivity Patterns

Connectivity-based parcellation has been previously used to identify clusters with distinct connectivity in the medial premotor wall [Johansen-Berg et al., 2004; Klein et al., 2007], in the IFG [Anwander et al., 2007; Klein et al., 2007], in the cingulate cortex [Beckmann et al., 2009], and in the lateral premotor cortex [Tomassini et al., 2007], whose boundaries were consistent with available cytoarchitectonic atlases and with results from animal studies. In these studies, spectral reordering [Barnard et al., 1995] or k-means clustering [Hartigan and Wong, 1979; Hartigan, 1975] were used, because a sharp segregation between clusters with distinct connectivity was expected on the basis of previous evidence from tracer-injection studies in macaques [Behrens and Johansen-Berg, 2005]. Accordingly, the relevant question was *where* the boundaries separating different clusters are located in humans. However, hard clustering cannot examine *whether* it is appropriate to assume that the data contain distinct clusters. In the case of the insula, several animal studies suggest a gradual rather than abrupt variation in connectivity: the gradient of increasingly more complex architecture spanning from agranular to granular territories [Friedman et al., 1986; Jones and Burton, 1976; Mesulam and Mufson, 1982a; Mesulam and Mufson, 1985; von Economo, 1927] appears to be related to the gradual change in connectivity patterns, as reported by tracer-injection studies [Amaral and Price, 1984; Chikama et al., 1997; Friedman et al., 1986; Fudge et al., 2005]. On other hand, a very recent study on the cytoarchitecture of the posterior human insula reported the presence of clear boundaries between granular and dysgranular insular regions [Kurth et al., 2010a]. Neuroimaging studies are only beginning to be able to detect differences among different cytoarchitectonic fields in vivo [Eickhoff et al., 2005a; Fatterpekar et al., 2002; Geyer et al., 2011], and, in the present study, we were not in the position to investigate the relative smoothness of the transition across cortical types in the insula. We instead used the results from probabilistic tractography (1) to investigate the likelihood of either a sharp (clustered) or a gradual transition among connectivity patterns and (2) to compare the relative sharpness of this transition with another brain region (mPMC) where sharply segregated clusters of connectivity patterns were shown in previous studies.

In a previous study using repeated *k*-means clustering, we showed that applying hard clustering to the cross-correlation matrix of connectivity patterns is undesirable in the insula: repeated application of *k*-means clustering reveals that in comparison with the mPMC, a significantly higher proportion of the middle insula cannot be reliably categorized using this method [Nanetti et al., 2009]. In this work, we therefore applied LE [Belkin and Niyogi, 2002] in order to analyze *how* the connectivity of the insula varies across different territories. Given the connectivity map of each seed voxel, which is the output of probabilistic tractography, this algorithm uses the information about the similarity between each and every other connectivity map to recover, if present, the main trajectories of connectivity variation across different territories of the seed region. In the case of the insula, several anatomical studies suggested that the main trajectory of connectivity variation would be topographically localized along the rostrocaudal anatomical axis and that the variation across connectivity patterns of different insular territories would be gradual rather than abrupt. We therefore expected LE to represent the change in connectivity patterns as a one-dimensional structure with relatively small interruptions, especially compared to other cortical regions where the change in connectivity is more sharp. In the latter case, we expected to detect relatively bigger gaps in the structure of connectivity variability recovered by LE. Note that while preventing artifactual clustering not supported by the data, this algorithm is nonetheless capable of revealing clusters when present [Belkin and Niyogi, 2002] and does not require an a priori hypothesis about the number of clusters. Additional precautions were also taken to avoid that the results of LE could be affected by the mere anatomical distance within seed voxels as well as between seed and target voxels. Specifically, (1) we corrected the count of the samples in each target voxel by the mean length of the pathways connecting each seed with each target voxel to ensure that the results of tractography would have not been biased toward anatomically close target voxels. The same correction was used for this reason in connectivity-based parcellation/classification studies [Beckmann et al., 2009; Eickhoff et al., 2010; Tomassini et al., 2007]. (2) An Euclidean anatomical distance matrix was added to the correlation/similarity matrix of the connectivity maps to penalize the similarity between seed voxels, which are very close in the anatomy. This prevents that the connectivity maps of two seed voxels would be quantified as similar in the LE just because of their anatomical proximity. (3) Also, potentially outlier points produced by an initial LE were removed prior to any analysis of the rate of change of connectivity to avoid the possibility that continuity could be suggested by the presence of noise (see Supporting Information: Theory and implementation of LE).

Applying this methods to the results of probabilistic tractography from the insula revealed a trajectory of variability between two extremes featuring very different connectivity maps. Examining the spatial location of this trajectory on the insular surface revealed that these extremes were located in the anterior dorsal and ventral insula and in the dorsal and posterior part of the long insular gyri, respectively. Visual inspection of the LE suggested that this change of connectivity was gradual rather than abrupt. To assess this graduality quantitatively, we compared this profile with that obtained by applying the same technique to the mPMC. We found that LE also revealed a one-dimensional structure of connectivity change in the mPMC, corresponding the the

rostrocaudal anatomical axis. However, the change of connectivity was significantly more gradual in the case of the insula, while that in the mPMC was characterized by the presence of larger "gaps" that are consistent with the results of hard clustering methods (see Fig. 5) [Anwander et al., 2007; Johansen-Berg et al., 2004; Klein et al., 2007; Nanetti et al., 2009]. These results contribute to our understanding of the connectivity of the insula in humans and suggest that LE (and possibly other methods for nonlinear dimensionality reduction, see Saul et al. [2005] for a review) can be useful in analyzing the connectivity structure of different regions in the brain, including those where the transition between different types of connectivity is not sharp.

Given the present results as well as the evidence from animal studies, it comes natural to ask how a gradual transition in connectivity could relate to the integrative functionality of the insular cortex. In a classical work, Mesulam and Mufson noted that "the insula as well as the adjacent orbitofrontal and temporopolar areas are characterized by a remarkable heterogeneity in cortical architecture, connectivity, and physiology. This heterogeneity which is a hallmark of paralimbic (mesocortical) parts of the brain, indicates neither a chaotic organization nor a haphazard distribution of behavioral specialization. Instead, evidence indicates that the insula, like other components of the paralimbic brain, acts as a multipurpose region of cortex were a remarkably wide range of neural processes modulate behaviors which primarily depend on interactions between the extrapersonal world and the internal milieu" [Mesulam and Mufson, 1985]. These considerations were substantialized during the following decades of functional neuroimaging works: recently, Craig [2009], while detailing his model of human awareness, proposed that a complete representation of all salient information for the organism at a given time is produced in a posterior-to-anterior progression in the insula by means of a progressive integration of "homeostatic conditions with the sensory environment, and with motivational, hedonic and social conditions in other parts of the brain" [Craig, 2009]. In a recent meta-analysis, Kurth et al. [2010b] focused on both functional integration and functional specialization in the insula: in all the examined functional domain, the regions that showed a specific effect to a certain functional category were substantially smaller than the regions involved in multiple different categories. The authors comment this evidence as an indication that the insula is characterized both by functional specialization and functional integration. Interestingly, several of the regions identified with the meta-analysis of functional integration span different territories featuring different cytoarchitecture, according to the available maps, and, according to our results, progressively different connectional fingerprints. In the same work, Kurth and colleagues propose that the presence of intrainsular connections and the evidence of overlap between functional categories in the anterior dorsal insula could be two possible ways of reasoning about how functional integration could be embodied in the insula. It is outside the scope of this work to define the most plausible or efficient hodological model for functional integration in the cortex; however, we speculate that the relatively gradual shift in connectivity patterns, which was recovered in the insula, would be consistent with the concept of a cortical region whose nature is fundamentally integrative, because such a region should have the capability of both receiving different sources of information (interoceptive, sensory, emotional, and cognitive), and the different aspects of them (for instance the physical and affective components of touch), abstracting them from their original domain and finally integrating them according to their saliency for the present situation that the organism has to cope with. Sharp functional subdivisions are usually accompanied by sharp transition of connectivity, like in the mPMC, while the integrative role of a region such as the insula could be better substantialized by the close proximity of different territories with slightly different, nevertheless similar or related, connectivity and functionality, sensitive to different aspects of the processed information. This is indeed the situation suggested on a regional scale by the present findings obtained with LE, at the spatial resolution allowed by in vivo DWI, as well as by previous studies in macaques, and in particular regarding insular connections with the amygdala [Amaral and Price, 1984] and the basal ganglia [Chikama et al., 1997; Fudge et al., 2005]. The same situation is suggested when looking at the segregation of whole brain projections from either the mPMC or the insula: SMA and preSMA (F3 and F6) contain markedly different connectivity with the rest of the brain and relatively modest connections among each other [Luppino, 1993]; on the other side, as we highlighted in the introduction, dysgranular territories of the insula project to regions in the brain that are also targeted by agranular and granular territories, and their differential connectivity is reflected in their topographical proximity with either agranular or granular insular territories.

Comparison with Functional Studies

Insula and speech articulation

Many studies reported an involvement of the left anterior insula in overt language production tasks and specifically in the motor control of speech [Ackermann and Riecker, 2004, 2010; Bamiou et al., 2003; Blank et al., 2002; Duffau et al., 2000; Price, 2000; Riecker et al., 2005; Saur et al., 2006; Wise et al., 1999]. Deficits in speech coordination are associated with lesions [Dronkers, 1996] and hypometabolism [Nestor et al., 2003] in the short gyri of the insula, and its activity increases as a function of syllabic complexity and sequence complexity during a polysyllabic items production task [Bohland and Guenther, 2006]. In the perceptual domain, the activity of the left anterior insula is positively (left hemisphere) or negatively (right

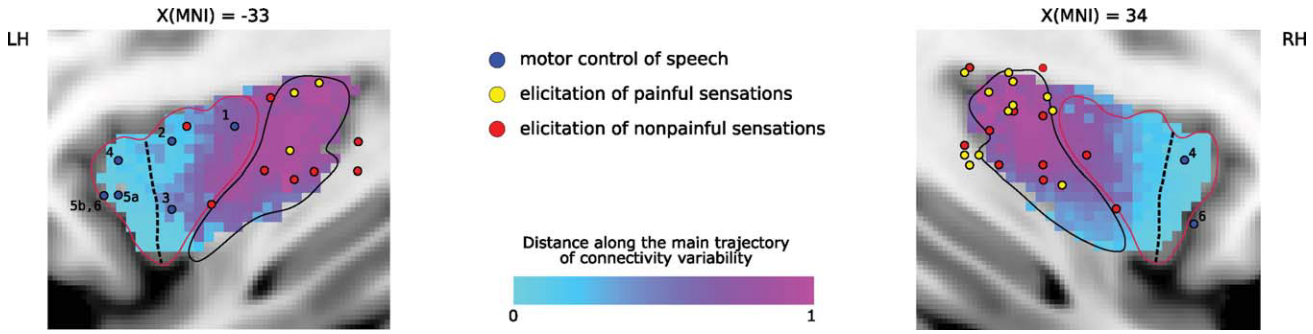

Figure 8.

Comparison with functional studies. The average trajectory of connectivity variability is overlaid onto the MNI single subject template. Only voxels belonging to at least half of the participants (five subjects) are mapped. Blue dots indicate the *y* and *z* coordinates of the local maxima for fMRI studies on motor control of speech in the following studies: (1) Dronkers [1996], (2) Blank et al. [2002], (3) Nestor et al. [2003], (4) Plante et al. [2006], (5a) and (5b) Saur et al. [2006], and (6) Geiser et al. [2008]. These locations are all in the insular territories where the strongest projections to BA44, BA45, and BA6 were found (see Fig. 6). Red and yellow dots indicate the locations from Ostrowsky et al. [2002] where intracortical stimulations elicited either painful (yellow) or nonpainful (red) sensations. Note the prevalent location in the long gyri of the insula, which we found to have maximum connection probability with somatosensory and posterior parietal regions (see Fig. 6). The meta-analysis of Schweinhardt et al. [2006] identified in the rostral anterior insula (rAI), caudally delimited by the short insular sulcus (dashed black line), as specifically involved in clinical pain with respect to nociceptive (experimental) pain, involving more posterior insular regions. The limbic lobe was found in the present study to receive projections mostly from the same insular territories (anterior short gyrus and ventral anterior insula—see Fig. 6). [Color figure can be viewed in the online issue, which is available at wileyonlinelibrary.com.]

hemisphere) correlated with the presentation rate of trains of clicks or syllables [Ackermann et al., 2001], while this effect is not present in patients with developmental dyslexia [Steinbrink et al., 2009]. Also, both the left anterior insula and BA44/45 in the IFG are involved in detecting pure rhythmic aspects of speech production [Geiser et al., 2008] as well as in recognizing degraded statements on the basis of their prosodic profile [Plante et al., 2006]. The fact that these anterior regions of the insula are more involved in language functions is compatible with the fact that this insular territory had the highest connection probability with the key frontal language regions (BA44, BA45, and BA6; see Fig. 6) in our study.

Insula and pain

The insula has been considered to be a core region for the integration of affective, empathic, interoceptive, and somatosensory components of pain [Brooks and Tracey, 2007; Lamm and Singer, 2010] with the insula being the most frequently reported brain region in pain-related fMRI experiments (see Apkarian et al. [2005] for a review). Two themes emerge from this vast number of publications: first, the rostral short gyri of the insula (rAI) seem to be most involved in the affective component of pain [Hein and Singer, 2008; Schweinhardt et al., 2006; Singer et al., 2004]; second, more posterior territories of the insula represent the sensory aspects of pain, with activity in these regions correlating with the physical properties of the stimulus [Frot et al., 2007] and electrostimulations determining sensory (tactile or nociceptive) qualia [Ostrowsky et al., 2002] (see Fig. 8). These findings are compatible with our results. First, in our study, we recorded the strongest connectivity to the limbic ROI (amygdala, EC, and hippocampus) in the most ventral anterior insula, and, to a lesser extent, in the entire anterior short gyrus and in the middle ventral insula. Second, the regions we found to be most connected with somatosensory and posterior parietal cortices were located in the posterior short gyrus and in the long insular gyri, which correspond to the regions found to be mostly involved in processing the physical properties of the stimulus (see Fig. 8).

Connection probability and functional organization of the insular cortex

In addition to the above considerations regarding speech articulation and pain, we report the results of two recent meta-analyses [Kurth et al., 2010b; Mutschler et al., 2009] performed on results from functional neuroimaging studies, in order to show the relationship of those findings with the results of our connectivity-based classification.

Mutschler and colleagues [Mutschler et al., 2009] performed a meta-analysis of the functional organization of the anterior insula using the results of 58 studies reporting 149 coordinates. The considered studies included auditory

and language processing, motor tasks involving upper and lower limbs, responses related to peripheral autonomic changes as well as tasks resulting in co-activation of the insula with the amygdala. The resulting maps are shown in Figure 6 (B1-B3) to appreciate the topographical relationship between functional specialization and peaks of connection probability. The functional meta-analysis map considering peripheral and autonomic changes as well as co-activation with the amygdala is localized in the anterior ventral insula, very close to the region where we found the peak for the connection probability with the limbic ROI (encompassing amygdala, EC, and hippocampus). The functional map considering studies on auditory and language processing is completely enclosed in the insular regions, where maximum connection probability was found with BA44 and BA45. Finally, the peak of the meta-analysis for studies on motor activity was located in a specific territory in the middle insula, in the ventral part of the posterior short gyrus, and to a lesser extent in the middle short gyrus, in the same locations, where we found connection probability values with the premotor cortex (BA6).

Kurth et al. [2010b] performed a meta-analysis on the coordinates obtained from 1768 experiments and collected in the BrainMap database [Fox et al., 2005b; Laird et al., 2005, 2009] and Pubmed. In this study, the authors investigated both functional integration and functional differentiations in the insula in 13 different functional categories (see Kurth et al. [2010b], Table 1). When combining these categories into four functional domains (sensorimotor, cognitive, chemical sensory, and social-emotional), the insula displayed a domain-specific functional organization, which mostly matches our results obtained by connectivity-based parcellation, in particular when relating BA44 and BA45 to the language-cognitive domain, the connection probability with the Limbic ROI to the social-emotional domain, and the connection probability with BA6 and SI to the somatosensory domain. In sum, these comparisons increases our confidence in the results obtained by performing in vivo probabilistic tractography of the insula and supports the hypothesis that the differential connectivity and the differential cytoarchitecture of the insula represents the substrate of the functional specialization of different insular territories.

Parcellation of the insular cortex on the basis of resting state functional connectivity

Recently, two works [Cauda et al., 2011; Deen et al., in press] used resting resting-state functional MRI (RS fmri) to perform a voxelwise parcellation of the insula on the basis of the correlation between the time course of each insular voxel with that of each other voxel in the brain. This methodology aims at recovering the intrinsic functional architecture of the brain by looking at regions, which feature similar spontaneous fluctuations of the blood-oxigenated level dependent signal. In the study of Deen et al. [in press], *k*-means clustering was performed on the average correlation matrix of insular functional connectivity profiles across subjects, and the optimal number of *k* was set to 3. Two clusters were identified in the anterior insula, the third in the posterior insula. In the study of Cauda et al. [2011], fuzzy c-means clustering was performed for each subject independently, and the optimal number of clusters was quantitatively set to 2. The algorithm divided the insula in one anterior and one posterior cluster. Although the spatial consistency of the anterior cluster found in Cauda et al. [2011] with the two anterior clusters found by Deen et al. [2010] cannot be precisely assessed on the basis of the published data as well as the location of the recovered subdivision with respect to the sulcal anatomy, we note that in the study of Cauda et al. [2011], the region where an overlap between the two clusters was found is located approximately where our previous repeated *k*-means clustering study on tractography data. Nanetti et al. [2009] found the highest density of voxels that could not be reliably assigned to either clusters: in the middle and posterior short insular gyri and in the anterior part of the long insular gyri. This convergent result from two different imaging modalities suggests that voxels in this insular region feature a high uncertainty when clustering techniques are used for the purpose of parcellation.

The discrepancy in the optimal number of clusters found between the study of Cauda et al. [2011] and that of Deen et al. [2010] might be due to a number of factors. For instance, Cauda et al. [2011] used spatial smoothing to to increase local correlation across neighbouring voxels, which could have masked the differences between dorsal and ventral anterior insula, as found by Deen et al. [2010]; on the other side, Deen et al. [2010] averaged all the individual subjects' correlation matrices before performing *k*-means clustering, while performing clustering on the single-subject correlation matrices would have made possible to check the consistency of the spatial location of clusters in order to decide the appropriate number of *k* (as it was done by Beckmann et al. [2009]). Further investigations by means of other dimensionality reduction techniques, which do not require an a priori choice of the number of clusters, such as multidimensional scaling or also the LE used in this study, could also help to clarify this point. In addition, these techniques could give further insights regarding whether the region of uncertainty recovered by Cauda et al. [2011] reflects a situation where the transition between functionally different cortical territories is less abrupt than in other brain regions [Kim et al., 2010].

CONCLUSIONS

In vivo probabilistic tractography is a relatively recent field of research, which still suffers from many limitations including low-signal-to-noise ratio in the images, low spatial resolution, problems related to tracking fibres in regions of particular structural complexity. In addition, it

cannot discriminate between afferent and efferent projections, and the recorded number of samples in the target voxels can be influenced by the distance between seed and target as well as by the geometry of the pathways connecting seed and targets [Johansen-Berg and Behrens, 2006; Jones, 2008]. Because of these limitations, the golden standard for investigations in anatomical connectivity is still represented by tracer-injection studies in animals, and it is therefore wise at the moment to focus current probabilistic tractography studies on testing in humans specific hypotheses derived from animal evidence. Considering the macaque data as the basis for generating hypothesis and as a rough meter of the validity of the findings reduces the likelihood of errors. Where the two sources of information diverge, a species difference or a methodological limitation might exist. Disentangling those two possibilities is difficult at the current stage of methodological development. Keeping these caveats in mind, we used probabilistic tractography to examine for the first time the connectivity of the human insula in vivo. The hypotheses that guided our work were grounded on the evidence about a relation between connectivity and cytoarchitecture in macaques and about the similar topographic arrangement of the cytoarchitecture in human and macaque insula. Fiber tracking was performed with an algorithm capable of resolving two main fiber populations within a voxel [Behrens et al., 2007], and the number of tractography samples reaching each target voxel was corrected by the mean path length between seed and target, as in previous studies [Beckmann et al., 2009; Eickhoff et al., 2010; Tomassini et al., 2007]. By analyzing the results with LE, we recovered in the insula a trajectory of connectivity variability spanning the rostrocaudal anatomical axis. Also, the transition among connectivity patterns in the insula was significantly smoother than that in the mPMC. The brain regions reached by tractography from different insular territories were largely consistent with the available evidence from animal studies both in terms of specificity (i.e., lack of aberrant connections) and sensitivity (i.e., finding those connections known to exist), and further analysis of the tractography samples count in target voxels, as well as of the connection probability with cytoarchitectonically defined regions suggested the presence of a relationship between connectivity patterns and cytoarchitecture, as it was found to be the case in macaques. Preliminary results from our laboratory suggest that very similar results can be obtained by performing the same analyses on ex vivo high-resolution diffusion-weighted data from macaque (see Cerliani [2009] and Supporting Information Fig. S2).

Although the available in vivo tractography techniques are still far from achieving results comparable to those derived from invasive studies, our study represents a further confirmation that tractography techniques can be used to test specific anatomical hypotheses—such as the relative sharpness/smoothness of a transition between different connectivity patterns—when these can be formulated at a degree of resolution compatible with the current limitations of DW imaging and white-matter tractography. More generally, we hope that our results will significantly broaden the spectrum of tools to analyze the results of in vivo tractography. The hard-clustering methods that have been used so far required the experimenter to think about the anatomical configuration of a region in terms of distinct clusters with sharp borders. This limited the application of in vivo connectivity-based parcellation studies to structures where such clusters are to be expected. LE, on the other hand, provides the opportunity to first *examine* whether a region's connectivity pattern is best described in terms of clusters featuring sharper transitions, as for the mPMC, or in terms of a more gradual transition, as for the insula. In the former case, Laplacian eigenmaps are useful to help estimating the number of clusters to ask to a clustering algorithm such as *k*-means. In the latter, it affords the possibility to describe the differences and similarities among the connectivity patterns of various territories of a brain region, without artificially dividing it into sharply segregated subregions, which could provide a suboptimal or incomplete representation of the intrinsic organization of the data.

ACKNOWLEDGMENTS

The authors thank Piray Atsak, James Augustine, Tim Behrens, Mikhail Belkin, Alberto Bizzi, Alex De Crespigny, Mbemba Jabbi Marsel Mesulam, Filippo Migliorati, Rudolf Nieuwenhuys, Steven Small, and Ana Solodkin for their encouragement and the important discussions during the realization of the work. Alfred Anwander and Frans Vanhoesel gave us very insightful advices for the preparation of the images. We owe a lot to our colleagues at the NIC: Anita Kuipers, Hans Hoogduin (now at UMC Utrecht) and Remco Renken for their precious competence in designing and optimizing MR sequences and acquiring images, Siemen Sikkema for his optimization of the algorithm for the computation of the cross-correlation matrix, and Harma Meffert for her help in acquiring the data. A particular acknowledgment goes to Mikhail Belkin for the important advices on the methodology of Laplacian Eigenmaps and for providing the code to compute them, to Isabella Mutschler and Tonio Ball for providing high-resolution images of the meta-analysis performed by them on functional studies in the insula, as well as for interesting suggestions and discussions on the present work, and to Simon Eickhoff for providing us the probabilistic cytoarchitectonic maps for the posterior parietal lobe. The authors declare no conflicts of interest.

REFERENCES

Ackermann H, Riecker A (2004): The contribution of the insula to motor aspects of speech production: A review and a hypothesis. Brain Lang 89:320–328.

Ackermann H, Riecker A (2010): The contribution(s) of the insula to speech production: A review of the clinical and functional imaging literature. Brain Struct Funct 214:419–433.

Ackermann H, Riecker A, Mathiak K, Erb M, Grodd W, Wildgruber D (2001): Rate-dependent activation of a prefrontal-insular-cerebellar network during passive listening to trains of click stimuli: An fMRI study. Neuroreport 12:4087–4092.

Afif A, Mertens P (2010): Description of sulcal organization of the insular cortex. Surg Radiol Anat 32:491–498.

Aggleton JP, Burton MJ, Passingham RE (1980): Cortical and subcortical afferents to the amygdala of the rhesus monkey (*Macaca mulatta*). Brain Res 190:347–368.

Allman JM, Tetreault NA, Hakeem AY, Manaye KF, Semendeferi K, Erwin JM, Park S, Goubert V, Hof PR (2010): The von Economo neurons in frontoinsular and anterior cingulate cortex in great apes and humans. Brain Struct Funct 214:495–517.

Amaral DG, Price JL (1984): Amygdalo-cortical projections in the monkey (*Macaca fascicularis*). J Comp Neurol 230:465–496.

Amunts K, Schleicher A, Burgel U, Mohlberg H, Uylings HB, Zilles K (1999): Broca's region revisited: Cytoarchitecture and intersubject variability. J Comp Neurol 412:319–341.

Amunts K, Weiss PH, Mohlberg H, Pieperhoff P, Eickhoff S, Gurd JM, Marshall JC, Shah NJ, Fink GR, Zilles K (2004): Analysis of neural mechanisms underlying verbal fluency in cytoarchitectonically defined stereotaxic space—The roles of Brodmann areas 44 and 45. Neuroimage 22:42–56.

Amunts K, Kedo O, Kindler M, Pieperhoff P, Mohlberg H, Shah NJ, Habel U, Schneider F, Zilles K (2005): Cytoarchitectonic mapping of the human amygdala, hippocampal region and entorhinal cortex: Intersubject variability and probability maps. Anat Embryol (Berl) 210:343–352.

Andersen RA, Asanuma C, Essick G, Siegel RM (1990): Corticocortical connections of anatomically and physiologically defined subdivisions within the inferior parietal lobule. J Comp Neurol 296:65–113.

Anwander A, Tittgemeyer M, von Cramon DY, Friederici AD, Knosche TR (2007): Connectivity-based parcellation of Broca's area. Cereb Cortex 17:816–825.

Apkarian AV, Bushnell MC, Treede RD, Zubieta JK (2005): Human brain mechanisms of pain perception and regulation in health and disease. Eur J Pain 9:463–484.

Augustine JR (1985): The insular lobe in primates including humans. Neurol Res 7:2–10.

Augustine JR (1996): Circuitry and functional aspects of the insular lobe in primates including humans. Brain Res Brain Res Rev 22:229–244.

Aziz-Zadeh L, Sheng T, Gheytanchi A (2010): Common premotor regions for the perception and production of prosody and correlations with empathy and prosodic ability. PLoS One 5:e8759.

Baier B, Karnath HO (2008): Tight link between our sense of limb ownership and self-awareness of actions. Stroke 39:486–488.

Bamiou DE, Musiek FE, Luxon LM (2003): The insula (Island of Reil) and its role in auditory processing. Literature review. Brain Res Brain Res Rev 42:143–154.

Barnard ST, Pothen A, Simon HD (1995): A spectral algorithm for envelope reduction of sparse matrices. Numer Linear Algebra Appl 2:317–334.

Beckmann M, Johansen-Berg H, Rushworth MF (2009): Connectivity-based parcellation of human cingulate cortex and its relation to functional specialization. J Neurosci 29:1175–1190.

Behrens TE, Johansen-Berg H (2005): Relating connectional architecture to grey matter function using diffusion imaging. Philos Trans R Soc Lond B Biol Sci 360:903–911.

Behrens TE, Woolrich MW, Jenkinson M, Johansen-Berg H, Nunes RG, Clare S, Matthews PM, Brady JM, Smith SM (2003): Characterization and propagation of uncertainty in diffusion-weighted MR imaging. Magn Reson Med 50:1077–1088.

Behrens TE, Berg HJ, Jbabdi S, Rushworth MF, Woolrich MW (2007): Probabilistic diffusion tractography with multiple fibre orientations: What can we gain? Neuroimage 34:144–155.

Belkin M, Niyogi P (2002): Laplacian eigenmaps and spectral techniques for embedding and clustering. In: Dietterich GT, Becker S, Ghahramani Z, editors. Advances in Neural Information Processing Systems. Cambridge: MIT Press. pp 585–591.

Belmalih A, Borra E, Contini M, Gerbella M, Rozzi S, Luppino G (2007): A multiarchitectonic approach for the definition of functionally distinct areas and domains in the monkey frontal lobe. J Anat 211:199–211.

Blank SC, Scott SK, Murphy K, Warburton E, Wise RJ (2002): Speech production: Wernicke, Broca and beyond. Brain 125:1829–1838.

Bohland JW, Guenther FH (2006): An fMRI investigation of syllable sequence production. Neuroimage 32:821–841.

Bonthius DJ, Solodkin A, Van Hoesen GW (2005): Pathology of the insular cortex in Alzheimer disease depends on cortical architecture. J Neuropathol Exp Neurol 64:910–922.

Brand S (1981): A serial section Golgi analysis of the primate claustrum. Anat Embryol (Berl) 162:475–488.

Brockhaus H (1940): Die Cyto- und Myeloarchitektonik des Cortex claustralis und des Claustrum beim Menschen. J Psychol Neurol 49:249–348.

Brodmann K (1909): Vergleichende Lokalisationslehre der Grosshirnrinde in ihren Prinzipien dargestellt aud Grund des Zellenbaues. JA Barth: Leipzig.

Brooks JC, Tracey I (2007): The insula: A multidimensional integration site for pain. Pain 128:1–2.

Butti C, Hof PR (2010): The insular cortex: A comparative perspective. Brain Struct Funct 214:477–493.

Carmichael ST, Clugnet MC, Price JL (1994): Central olfactory connections in the macaque monkey. J Comp Neurol 346:403–434.

Caspers S, Geyer S, Schleicher A, Mohlberg H, Amunts K, Zilles K (2006): The human inferior parietal cortex: Cytoarchitectonic parcellation and interindividual variability. Neuroimage 33:430–448.

Catani M, Howard RJ, Pajevic S, Jones DK (2002): Virtual in vivo interactive dissection of white matter fasciculi in the human brain. Neuroimage 17:77–94.

Cauda F, D'Agata F, Sacco K, Duca S, Geminiani G, Vercelli A (2011): Functional connectivity of the insula in the resting brain. Neuroimage 55:8–23.

Cavada C, Goldman-Rakic PS (1989): Posterior parietal cortex in rhesus monkey. I. Parcellation of areas based on distinctive limbic and sensory corticocortical connections. J Comp Neurol 287:393–421.

Cavada C, Company T, Tejedor J, Cruz-Rizzolo RJ, Reinoso-Suarez F (2000): The anatomical connections of the macaque monkey orbitofrontal cortex. A review. Cereb Cortex 10:220–242.

Cereda C, Ghika J, Maeder P, Bogousslavsky J (2002): Strokes restricted to the insular cortex. Neurology 59:1950–1955.

Cerliani L (2009): Trajectories of connectivity variation in the macaque insula recovered by means of probabilistic white

matter tractography on diffusion-weighted magnetic resonance data. SfN Society for Neuroscience Conference, Chicago.
Chikama M, McFarland NR, Amaral DG, Haber SN (1997): Insular cortical projections to functional regions of the striatum correlate with cortical cytoarchitectonic organization in the primate. J Neurosci 17:9686–9705.
Craig AD (2005): Forebrain emotional asymmetry: A neuroanatomical basis? Trends Cogn Sci 9:566–571.
Craig AD (2009): How do you feel now? The anterior insula and human awareness. Nat Rev Neurosci 10:59–70.
Craig AD (2010): The sentient self. Brain Struct Funct 214:563–577.
Crick FC, Koch C (2005): What is the function of the claustrum? Philos Trans R Soc Lond B Biol Sci 360:1271–1279.
Croxson PL, Johansen-Berg H, Behrens TE, Robson MD, Pinsk MA, Gross CG, Richter W, Richter MC, Kastner S, Rushworth MF (2005): Quantitative investigation of connections of the prefrontal cortex in the human and macaque using probabilistic diffusion tractography. J Neurosci 25:8854–8866.
Darian-Smith C, Darian-Smith I, Burman K, Ratcliffe N (1993): Ipsilateral cortical projections to areas 3a, 3b, and 4 in the macaque monkey. J Comp Neurol 335:200–213.
Deen B, Pitskel NB, Pelphrey KA (2010): Three systems of insular functional connectivity identified with cluster analysis. Cereb Cortex. [Epub ahead of print].
Dronkers NF (1996): A new brain region for coordinating speech articulation. Nature 384:159–161.
Duffau H, Capelle L, Lopes M, Faillot T, Sichez JP, Fohanno D (2000): The insular lobe: Physiopathological and surgical considerations. Neurosurgery 47:801–810; discussion 810–811.
Eickhoff S, Walters NB, Schleicher A, Kril J, Egan GF, Zilles K, Watson JD, Amunts K (2005a): High-resolution MRI reflects myeloarchitecture and cytoarchitecture of human cerebral cortex. Hum Brain Mapp 24:206–215.
Eickhoff SB, Stephan KE, Mohlberg H, Grefkes C, Fink GR, Amunts K, Zilles K (2005b) A new SPM toolbox for combining probabilistic cytoarchitectonic maps and functional imaging data. Neuroimage 25:1325–1335.
Eickhoff SB, Jbabdi S, Caspers S, Laird AR, Fox PT, Zilles K, Behrens TE (2010): Anatomical and functional connectivity of cytoarchitectonic areas within the human parietal operculum. J Neurosci 30:6409–6421.
Fatterpekar GM, Naidich TP, Delman BN, Aguinaldo JG, Gultekin SH, Sherwood CC, Hof PR, Drayer BP, Fayad ZA (2002): Cytoarchitecture of the human cerebral cortex: MR microscopy of excised specimens at 9.4 Tesla. AJNR Am J Neuroradiol 23:1313–1321.
Fernandez-Miranda JC, Rhoton ALJ, Kakizawa Y, Choi C, Alvarez-Linera J (2008): The claustrum and its projection system in the human brain: A microsurgical and tractographic anatomical study. J Neurosurg 108, 764–774.
Fox MD, Snyder AZ, Vincent JL, Corbetta M, Van Essen DC, Raichle ME (2005a) The human brain is intrinsically organized into dynamic, anticorrelated functional networks. Proc Natl Acad Sci USA 102:9673–9678.
Fox PT, Laird AR, Fox SP, Fox PM, Uecker AM, Crank M, Koenig SF, Lancaster JL (2005b) BrainMap taxonomy of experimental design: Description and evaluation. Hum Brain Mapp 25:185–198.
Friedman DP, Murray EA, O'Neill JB, Mishkin M (1986): Cortical connections of the somatosensory fields of the lateral sulcus of macaques: Evidence for a corticolimbic pathway for touch. J Comp Neurol 252:323–347.
Frot M, Magnin M, Mauguiere F, Garcia-Larrea L (2007): Human SII and posterior insula differently encode thermal laser stimuli. Cereb Cortex 17:610–620.
Fudge JL, Breitbart MA, Danish M, Pannoni V (2005): Insular and gustatory inputs to the caudal ventral striatum in primates. J Comp Neurol 490:101–118.
Geiser E, Zaehle T, Jancke L, Meyer M (2008): The neural correlate of speech rhythm as evidenced by metrical speech processing. J Cogn Neurosci 20:541–552.
Gerbella M, Belmalih A, Borra E, Rozzi S, Luppino G (2007): Multimodal architectonic subdivision of the caudal ventrolateral prefrontal cortex of the macaque monkey. Brain Struct Funct 212:269–301.
Gerbella M, Belmalih A, Borra E, Rozzi S, Luppino G (2010): Cortical connections of the macaque caudal ventrolateral prefrontal areas 45A and 45B. Cereb Cortex 20:141–168.
Geyer S (2004): The microstructural border between the motor and the cognitive domain in the human cerebral cortex. Adv Anat Embryol Cell Biol 174:I-VIII, 1–89.
Geyer S, Schleicher A, Zilles K (1999): Areas 3a, 3b, and 1 of human primary somatosensory cortex. Neuroimage 10:63–83.
Geyer S, Matelli M, Luppino G, Zilles K (2000): Functional neuroanatomy of the primate isocortical motor system. Anat Embryol (Berl) 202:443–474.
Geyer S, Weiss M, Reimann K, Lohmann G, Turner R (2011): Microstructural parcellation of the human cerebral cortex—From Brodmann's post-mortem map to *in vivo* mapping with high-field magnetic resonance imaging. Front Hum Neurosci 5:1–7.
Grefkes C, Geyer S, Schormann T, Roland P, Zilles K (2001): Human somatosensory area. II. Observer-independent cytoarchitectonic mapping, interindividual variability, and population map. Neuroimage 14:617–631.
Hartigan JA (1975): Clustering Algorithms. Wiley: New York, NY.
Hartigan JA, Wong MA (1979): A k-means clustering agorithm. Appl Stat 28:100–108.
Heimer L, Van Hoesen GW (2006): The limbic lobe and its output channels: Implications for emotional functions and adaptive behavior. Neurosci Biobehav Rev 30:126–147.
Hein G, Singer T (2008): I feel how you feel but not always: The empathic brain and its modulation. Curr Opin Neurobiol 18:153–158.
Holmes CJ, Hoge R, Collins L, Woods R, Toga AW, Evans AC (1998): Enhancement of MR images using registration for signal averaging. J Comput Assist Tomogr 22:324–333.
Ibanez A, Gleichgerrcht E, Manes F (2010): Clinical effects of insular damage in humans. Brain Struct Funct 214:397–410.
Iturria-Medina Y, Fernandez AP, Morris DM, Canales-Rodriguez EJ, Haroon HA, Penton LG, Augath M, Garcia LG, Logothetis N, Parker GJ, Melie-Garcia L (2011): Brain hemispheric structural efficiency and interconnectivity rightward asymmetry in human and nonhuman primates. Cereb Cortex 21:56–67.
Jabbi M, Swart M, Keysers C (2007): Empathy for positive and negative emotions in the gustatory cortex. Neuroimage 34: 1744–1753.
Jenkinson M, Bannister P, Brady M, Smith S (2002): Improved optimization for the robust and accurate linear registration and motion correction of brain images. Neuroimage 17:825–841.
Johansen-Berg H, Behrens TE (2006): Just pretty pictures? What diffusion tractography can add in clinical neuroscience. Curr Opin Neurol 19:379–385.

Johansen-Berg H, Behrens TE, Robson MD, Drobnjak I, Rushworth MF, Brady JM, Smith SM, Higham DJ, Matthews PM (2004): Changes in connectivity profiles define functionally distinct regions in human medial frontal cortex. Proc Natl Acad Sci USA 101:13335–13340.

Johansen-Berg H, Gutman DA, Behrens TE, Matthews PM, Rushworth MF, Katz E, Lozano AM, Mayberg HS (2008): Anatomical connectivity of the subgenual cingulate region targeted with deep brain stimulation for treatment-resistant depression. Cereb Cortex 18:1374–1383.

Johnson JI, Buchanann KJ, Morris JA, Fobbs AJJ (2009): Interrelation of gyral formation, cytoarchitectural variations, and sensory regions in human insular cortex. SfN Society for Neuroscience Conference, Chicago.

Jones DK (2008): Studying connections in the living human brain with diffusion MRI. Cortex 44:936–952.

Jones EG, Burton H (1976): Areal differences in the laminar distribution of thalamic afferents in cortical fields of the insular, parietal and temporal regions of primates. J Comp Neurol 168:197–247.

Karnath HO, Baier B (2010): Right insula for our sense of limb ownership and self-awareness of actions. Brain Struct Funct 214:411–417.

Karnath HO, Baier B, Nagele T (2005): Awareness of the functioning of one's own limbs mediated by the insular cortex? J Neurosci 25:7134–7138.

Kaufman JA, Paul LK, Manaye KF, Granstedt AE, Hof PR, Hakeem AY, Allman JM (2008): Selective reduction of Von Economo neuron number in agenesis of the corpus callosum. Acta Neuropathol 116:479–489.

Kerr KM, Agster KL, Furtak SC, Burwell RD (2007): Functional neuroanatomy of the parahippocampal region: The lateral and medial entorhinal areas. Hippocampus 17:697–708.

Kim JH, Lee JM, Jo HJ, Kim SH, Lee JH, Kim ST, Seo SW, Cox RW, Na DL, Kim SI, Saad ZS (2010): Defining functional SMA and pre-SMA subregions in human MFC using resting state fMRI: Functional connectivity-based parcellation method. Neuroimage 49:2375–2386.

Kleber B, Veit R, Birbaumer N, Gruzelier J, Lotze M (2010): The brain of opera singers: Experience-dependent changes in functional activation. Cereb Cortex 20:1144–1152.

Klein JC, Behrens TE, Robson MD, Mackay CE, Higham DJ, Johansen-Berg H (2007): Connectivity-based parcellation of human cortex using diffusion MRI: Establishing reproducibility, validity and observer independence in BA 44/45 and SMA/pre-SMA. Neuroimage 34:204–211.

Kondo H, Saleem KS, Price JL (2005): Differential connections of the perirhinal and parahippocampal cortex with the orbital and medial prefrontal networks in macaque monkeys. J Comp Neurol 493:479–509.

Kowianski P, Dziewiatkowski J, Kowianska J, Morys J (1999): Comparative anatomy of the claustrum in selected species: A morphometric analysis. Brain Behav Evol 53:44–54.

Kubicki M, Westin CF, Maier SE, Frumin M, Nestor PG, Salisbury DF, Kikinis R, Jolesz FA, McCarley RW, Shenton ME (2002): Uncinate fasciculus findings in schizophrenia: A magnetic resonance diffusion tensor imaging study. Am J Psychiatry 159:813–820.

Kurth F, Eickhoff SB, Schleicher A, Hoemke L, Zilles K, Amunts K (2010a) Cytoarchitecture and probabilistic maps of the human posterior insular cortex. Cereb Cortex 20:1448–1461.

Kurth F, Zilles K, Fox PT, Laird AR, Eickhoff SB (2010b) A link between the systems: Functional differentiation and integration within the human insula revealed by meta-analysis. Brain Struct Funct 214:519–534.

Laird AR, Lancaster JL, Fox PT (2005): BrainMap: The social evolution of a human brain mapping database. Neuroinformatics 3:65–78.

Laird AR, Eickhoff SB, Kurth F, Fox PM, Uecker AM, Turner JA, Robinson JL, Lancaster JL, Fox PT (2009): ALE meta-analysis workflows via the Brainmap database: Progress towards a probabilistic functional brain atlas. Front Neuroinform 3:1–11.

Lamm C, Singer T (2010): The role of anterior insular cortex in social emotions. Brain Struct Funct 214:579–591.

LeVay S, Sherk H (1981): The visual claustrum of the cat. I. Structure and connections. J Neurosci 1:956–980.

Luppino G, Matelli M, Camarda R, Rizzolatti G (1993): Corticocortical connections of area F3 (SMA-proper) and area F6 (pre-SMA) in the macaque monkey. J Comp Neurol 338:114–140.

Matelli M, Luppino G, Rizzolatti G (1985): Patterns of cytochrome oxidase activity in the frontal agranular cortex of the macaque monkey. Behav Brain Res 18:125–136.

Matelli M, Camarda R, Glickstein M, Rizzolatti G (1986): Afferent and efferent projections of the inferior area 6 in the macaque monkey. J Comp Neurol 251:281–298.

Mesulam MM, Mufson EJ (1982a) Insula of the old world monkey. I. Architectonics in the insulo-orbito-temporal component of the paralimbic brain. J Comp Neurol 212:1–22.

Mesulam MM, Mufson EJ (1982b) Insula of the old world monkey. III. Efferent cortical output and comments on function. J Comp Neurol 212:38–52.

Mesulam MM, Mufson EJ (1985): The insula of Reil in man and monkey. Architectonics, connectivity, and function. In: Jones P, editor. Cerebral Cortex. New York: Plenum.

Meyer M, Alter K, Friederici AD, Lohmann G, von Cramon DY (2002): FMRI reveals brain regions mediating slow prosodic modulations in spoken sentences. Hum Brain Mapp 17:73–88.

Mohedano-Moriano A, Pro-Sistiaga P, Arroyo-Jimenez MM, Artacho-Perula E, Insausti AM, Marcos P, Cebada-Sanchez S, Martinez-Ruiz J, Munoz M, Blaizot X, Martinez-Marcos A, Amaral DG, Insausti R (2007): Topographical and laminar distribution of cortical input to the monkey entorhinal cortex. J Anat 211:250–260.

Moran MA, Mufson EJ, Mesulam MM (1987): Neural inputs into the temporopolar cortex of the rhesus monkey. J Comp Neurol 256:88–103.

Morgane PJ, Mokler DJ (2006): The limbic brain: Continuing resolution. Neurosci Biobehav Rev 30:119–125.

Mufson EJ, Mesulam MM (1982): Insula of the old world monkey. II. Afferent cortical input and comments on the claustrum. J Comp Neurol 212:23–37.

Mufson EJ, Mesulam MM, Pandya DN (1981): Insular interconnections with the amygdala in the rhesus monkey. Neuroscience 6:1231–1248.

Mutschler I, Wieckhorst B, Kowalevski S, Derix J, Wentlandt J, Schulze-Bonhage A, Ball T (2009): Functional organization of the human anterior insular cortex. Neurosci Lett 457:66–70.

Naidich TP, Kang E, Fatterpekar GM, Delman BN, Gultekin SH, Wolfe D, Ortiz O, Yousry I, Weismann M, Yousry TA (2004): The insula: Anatomic study and MR imaging display at 1.5 T. AJNR Am J Neuroradiol 25:222–232.

Nanetti L, Cerliani L, Gazzola V, Renken R, Keysers C (2009): Group analyses of connectivity-based cortical parcellation using repeated k-means clustering. Neuroimage 47:1666–1677.

Neal JW, Pearson RC, Powell TP (1987): The cortico-cortical connections of area 7b, PF, in the parietal lobe of the monkey. Brain Res 419:341–346.

Nelissen K, Luppino G, Vanduffel W, Rizzolatti G, Orban GA (2005): Observing others: Multiple action representation in the frontal lobe. Science 310:332–336.

Nestor PJ, Graham NL, Fryer TD, Williams GB, Patterson K, Hodges JR (2003): Progressive non-fluent aphasia is associated with hypometabolism centred on the left anterior insula. Brain 126:2406–2418.

Nieuwenhuys R, Voogd J, Huijzen v (2008): The Human Central Nervous System. Springer-Verlag: Berlin.

Nimchinsky EA, Gilissen E, Allman JM, Perl DP, Erwin JM, Hof PR (1999): A neuronal morphologic type unique to humans and great apes. Proc Natl Acad Sci USA 96:5268–5273.

Oldfield RC (1971): The assessment and analysis of handedness: The Edinburgh inventory. Neuropsychologia 9:97–113.

Ongur D, Ferry AT, Price JL (2003): Architectonic subdivision of the human orbital and medial prefrontal cortex. J Comp Neurol 460:425–449.

Ostrowsky K, Magnin M, Ryvlin P, Isnard J, Guenot M, Mauguiere F (2002): Representation of pain and somatic sensation in the human insula: A study of responses to direct electrical cortical stimulation. Cereb Cortex 12:376–385.

Petrides M (2005): Lateral prefrontal cortex: Architectonic and functional organization. Philos Trans R Soc Lond B Biol Sci 360:781–795.

Petrides M (2006): Broca's area in the human and in the nonhuman brain. In: Grodzinsky Y, Amunts K, editors. Broca's Region. Oxford: Oxford University Press.

Petrides M, Pandya DN (1999): Dorsolateral prefrontal cortex: Comparative cytoarchitectonic analysis in the human and the macaque brain and corticocortical connection patterns. Eur J Neurosci 11:1011–1036.

Petrides M, Pandya DN (2002): Comparative cytoarchitectonic analysis of the human and the macaque ventrolateral prefrontal cortex and corticocortical connection patterns in the monkey. Eur J Neurosci 16:291–310.

Picard N, Strick PL (1996): Motor areas of the medial wall: A review of their location and functional activation. Cereb Cortex 6:342–353.

Plante E, Holland SK, Schmithorst VJ (2006): Prosodic processing by children: An fMRI study. Brain Lang 97:332–342.

Price CJ (2000): The anatomy of language: Contributions from functional neuroimaging. J Anat 197 (Pt 3):335–359.

Pritchard TC, Norgren R (2004): Gustatory system. In: Paxinos G, Mai JK, editors. The Human Nervous System. San Diego: Academic Press. pp 1171–1196.

Pritchard TC, Hamilton RB, Morse JR, Norgren R (1986): Projections of thalamic gustatory and lingual areas in the monkey, *Macaca fascicularis*. J Comp Neurol 244:213–228.

Riecker A, Ackermann H, Wildgruber D, Dogil G, Grodd W (2000): Opposite hemispheric lateralization effects during speaking and singing at motor cortex, insula and cerebellum. Neuroreport 11:1997–2000.

Riecker A, Mathiak K, Wildgruber D, Erb M, Hertrich I, Grodd W, Ackermann H (2005): fMRI reveals two distinct cerebral networks subserving speech motor control. Neurology 64:700–706.

Rizzolatti G, Arbib MA (1998): Language within our grasp. Trends Neurosci 21:188–194.

Rizzolatti G, Luppino G, Matelli M (1998): The organization of the cortical motor system: New concepts. Electroencephalogr Clin Neurophysiol 106:283–296.

Rodrigo S, Naggara O, Oppenheim C, Golestani N, Poupon C, Cointepas Y, Mangin JF, Le Bihan D, Meder JF (2007): Human subinsular asymmetry studied by diffusion tensor imaging and fiber tracking. AJNR Am J Neuroradiol 28:1526–1531.

Rose M (1928): Die Inselrinde des Menschen und der Tiere. J Psychol Neurol 37:467–624.

Rozzi S, Calzavara R, Belmalih A, Borra E, Gregoriou GG, Matelli M, Luppino G (2006): Cortical connections of the inferior parietal cortical convexity of the macaque monkey. Cereb Cortex 16:1389–1417.

Rushworth MF, Behrens TE, Johansen-Berg H (2006): Connection patterns distinguish 3 regions of human parietal cortex. Cereb Cortex 16:1418–1430.

Saul L, Weinberger K, Sha F, Ham J, Lee DD (2005): Spectral methods for dimensionality reduction. In: Schöelkopf B, Chapelle O, Zien A, editors. Semisupervised Learning. Boston, MA: MIT Press. pp 279–294.

Saur D, Lange R, Baumgaertner A, Schraknepper V, Willmes K, Rijntjes M, Weiller C (2006): Dynamics of language reorganization after stroke. Brain 129:1371–1384.

Scheperjans F, Eickhoff SB, Homke L, Mohlberg H, Hermann K, Amunts K, Zilles K (2008): Probabilistic maps, morphometry, and variability of cytoarchitectonic areas in the human superior parietal cortex. Cereb Cortex 18:2141–2157.

Schmahmann JD, Pandya DN (2007): The complex history of the fronto-occipital fasciculus. J Hist Neurosci 16:362–377.

Schmahmann JD, Pandya DN, Wang R, Dai G, D'Arceuil HE, de Crespigny AJ, Wedeen VJ (2007): Association fibre pathways of the brain: Parallel observations from diffusion spectrum imaging and autoradiography. Brain 130:630–653.

Schneider RJ, Friedman DP, Mishkin M (1993): A modality-specific somatosensory area within the insula of the rhesus monkey. Brain Res 621:116–120.

Schweinhardt P, Glynn C, Brooks J, McQuay H, Jack T, Chessell I, Bountra C, Tracey I (2006): An fMRI study of cerebral processing of brush-evoked allodynia in neuropathic pain patients. Neuroimage 32:256–265.

Seeley WW (2010): Anterior insula degeneration in frontotemporal dementia. Brain Struct Funct 214:465–475.

Seeley WW, Carlin DA, Allman JM, Macedo MN, Bush C, Miller BL, Dearmond SJ (2006): Early frontotemporal dementia targets neurons unique to apes and humans. Ann Neurol 60: 660–667.

Semendeferi K, Damasio H (2000): The brain and its main anatomical subdivisions in living hominoids using magnetic resonance imaging. J Hum Evol 38:317–332.

Shaw P, Kabani NJ, Lerch JP, Eckstrand K, Lenroot R, Gogtay N, Greenstein D, Clasen L, Evans A, Rapoport JL, Giedd JN, Wise SP (2008): Neurodevelopmental trajectories of the human cerebral cortex. J Neurosci 28:3586–3594.

Shipp S, Blanton M, Zeki S (1998): A visuo-somatomotor pathway through superior parietal cortex in the macaque monkey: Cortical connections of areas V6 and V6A. Eur J Neurosci 10:3171–3193.

Singer T, Seymour B, O'Doherty J, Kaube H, Dolan RJ, Frith CD (2004): Empathy for pain involves the affective but not sensory components of pain. Science 303:1157–1162.

Small DM (2010): Taste representation in the human insula. Brain Struct Funct 214:551–561.

Small DM, Zald DH, Jones-Gotman M, Zatorre RJ, Pardo JV, Frey S, Petrides M (1999): Human cortical gustatory areas: A review of functional neuroimaging data. Neuroreport 10:7–14.

Smith SM (2002): Fast robust automated brain extraction. Hum Brain Mapp 17:143–155.

Smith SM, Jenkinson M, Woolrich MW, Beckmann CF, Behrens TE, Johansen-Berg H, Bannister PR, De Luca M, Drobnjak I, Flitney DE, Niazy RK, Saunders J, Vickers J, Zhang Y, De Stefano N, Brady JM, Matthews PM (2004): Advances in functional and structural MR image analysis and implementation as FSL. Neuroimage 23 (Suppl 1):S208–S219.

Stefanacci L, Amaral DG (2002): Some observations on cortical inputs to the macaque monkey amygdala: An anterograde tracing study. J Comp Neurol 451:301–323.

Steinbrink C, Ackermann H, Lachmann T, Riecker A (2009): Contribution of the anterior insula to temporal auditory processing deficits in developmental dyslexia. Hum Brain Mapp 30:2401–2411.

Tanne-Gariepy J, Boussaoud D, Rouiller EM (2002): Projections of the claustrum to the primary motor, premotor, and prefrontal cortices in the macaque monkey. J Comp Neurol 454:140–157.

Tomassini V, Jbabdi S, Klein JC, Behrens TE, Pozzilli C, Matthews PM, Rushworth MF, Johansen-Berg H (2007): Diffusion-weighted imaging tractography-based parcellation of the human lateral premotor cortex identifies dorsal and ventral subregions with anatomical and functional specializations. J Neurosci 27:10259–10269.

Tsakiris M, Hesse MD, Boy C, Haggard P, Fink GR (2007): Neural signatures of body ownership: A sensory network for bodily self-consciousness. Cereb Cortex 17:2235–2244.

Ture U, Yasargil DC, Al-Mefty O, Yasargil MG (1999): Topographic anatomy of the insular region. J Neurosurg 90:720–733.

van den Heuvel MP, Mandl RC, Kahn RS, Hulshoff Pol HE (2009): Functionally linked resting-state networks reflect the underlying structural connectivity architecture of the human brain. Hum Brain Mapp 30:3127–3141.

Van Essen DC (2005): A population-average, landmark- and surface-based (PALS) atlas of human cerebral cortex. Neuroimage 28:635–662.

Van Essen DC, Drury HA, Dickson J, Harwell J, Hanlon D, Anderson CH (2001): An integrated software suite for surface-based analyses of cerebral cortex. J Am Med Inform Assoc 8:443–459.

Varnavas GG, Grand W (1999): The insular cortex: Morphological and vascular anatomic characteristics. Neurosurgery 44:127–136; discussion 136–138.

Veldhuizen MG, Rudenga K, Small DM (2008): The pleasure of taste, flavor and food. In: Berridge KC, Kringelbach ML, editors. The Neurobiology of Pleasure. Oxford: Oxford University Press.

Vogt C, Vogt O (1919): Allgemeinere ergebnisse unserer hinforschungen. J Psychol Neurol Leipzig 25:247–462.

von Economo C (1927): Zellaufbau der Grosshirnrinde des Menschen. Zehn Vorlesungen mit 61 Abbildungen. Springer: Berlin.

von Economo C, Koskinas GN (1925): Die Cytoarchitektonik der Hirnrinde des erwachsenen Menschen. Textband und Atlas mit 112 mikrophotographischen Tafeln. Springer: Wien.

Watkins KE, Paus T, Lerch JP, Zijdenbos A, Collins DL, Neelin P, Taylor J, Worsley KJ, Evans AC (2001): Structural asymmetries in the human brain: A voxel-based statistical analysis of 142 MRI scans. Cereb Cortex 11:868–877.

Wildgruber D, Hertrich I, Riecker A, Erb M, Anders S, Grodd W, Ackermann H (2004): Distinct frontal regions subserve evaluation of linguistic and emotional aspects of speech intonation. Cereb Cortex 14:1384–1389.

Wise RJ, Greene J, Buchel C, Scott SK (1999): Brain regions involved in articulation. Lancet 353:1057–1061.

Woolrich MW, Jbabdi S, Patenaude B, Chappell M, Makni S, Behrens T, Beckmann C, Jenkinson M, Smith SM (2009): Bayesian analysis of neuroimaging data in FSL. Neuroimage 45:S173–S186.

Zilles K (2004) Architecture of the human cerebral cortex. Regional and laminar organization. In: Paxinos G, Mai JK, editors. The Human Nervous System. San Diego: Academic Press. pp 997–1055.